PROSPECTS

IN PHARMACEUTICAL SCIENCES

Original Article

MOLECULAR DOCKING, BIOACTIVITY, ADME, TOXICITY RISKS, AND QUANTUM MECHANICAL PARAMETERS OF SOME 1,2-DIHYDROQUINOLINE DERIVATIVES WERE CALCULATED THEORETICALLY FOR INVESTIGATION OF ITS USE AS A PHARMACEUTICAL ACTIVE INGREDIENT IN THE TREATMENT OF MULTIPLE SCLEROSIS (MS)

Fatih İslamoğlu

Department of Chemistry, Recep Tayyip Erdoğan University, Rize 53100, Turkey

* Correspondence, e-mail: fatih.islamoglu@erdogan.edu.tr

ABSTRACT

In this study, some 1,2-dihydroquinoline derivatives, which have not been synthesized before, were designed, and their usability in the treatment of multiple sclerosis (MS) was investigated. Firstly, a docking study was conducted between the designed molecules and the target proteins (3PP4, 6OBD, 7YXA, and 7TD4) that interact with drugs (International Nonproprietary Name (INN): Ocrelizumab, Alemtuzumab, and Siponimod) used in the treatment of MS. ADME (absorption, distribution, metabolism, and excretion) properties (Boiled Egg graph, bioavailability radar, physicochemical properties, lipophilicity, water solubility, pharmacokinetics, drug similarity, and medicinal chemistry) were analyzed. Bioactivity score, drug-likeness score, drug score, toxicity risks (mutagenic, tumorigenic, irritant, reproductive effective, fathead minnow LC_{50} (96 hours), daphnia magna LC_{50} (48 hours), oral rat LD_{50}), bioconcentration factor, and density values were calculated. Quantum mechanical parameters include highest occupied molecular orbital energy (E_{HOMO}), lowest unoccupied molecular orbital energy (E_{LUMO}), chemical potential (μ), electron affinity (EA), global softness (S), global hardness (η), ionization potential (IP), total energy, dipole moments, and electrophilicity (ω) values were also calculated for all molecules. As a result of the data obtained from all these studies, (7-(diethylamino)-1,2-dihydroquinolin-3-yl)(6-(diethylamino)-2,3-dihydro-1*H*-indazol-1-yl)methanone was determined to be the most ideal molecule that can be used as a pharmaceutical active ingredient in the treatment of MS. Bond angles, bond lengths, Mulliken atomic charges, and molecular electrostatic potential (MEP) were calculated for this ideal molecule, and the structure of the molecule was explained in a multifaceted way.

KEYWORDS: 1,2-dihydroquinoline derivatives, molecular docking, multiple sclerosis, ADME, quantum mechanical parameters.

1. Introduction

Because of their variety of pharmacological actions, 1,2-dihydroquinoline derivatives are a significant family of molecules in medicinal chemistry [1–5]. Pharmaceutical research and development are quite interested in these compounds. There are many studies in the literature on the availability of 1,2-dihydroquinoline derivative compounds and their use as active ingredients in pharmaceuticals, especially those exhibiting various biological activities as antimicrobial [6], antimalarial [7], antiviral [8], anticancer [9], anti-inflammatory [10], and antioxidant [11]. Extensive chemical changes are possible thanks to the 1,2-dihydroquinoline scaffold, which can improve the pharmacological characteristics and selectivity of these compounds. Their structural adaptability renders them promising candidates for pharmaceutical development. While specific 1,2-dihydroquinoline derivatives as active pharmaceutical ingredients (APIs) in marketed drugs are not very common, some derivatives of dihydroquinolines in cancer therapy as kinase inhibitors [12] or modulators of other cancer-related pathways and dihydroquinolines in neuroprotection for their potential use in neurodegenerative diseases [13] due to their antioxidant properties have been investigated for their potential in various therapeutic areas. A chronic autoimmune illness that

affects the brain and spinal cord, MS is a condition that affects the central nervous system (CNS) [14]. A wide range of symptoms are caused by the illness, and each person's experience with severity and progression will differ greatly. The protective covering of nerve fibers called the myelin sheath is wrongly attacked by the immune system in MS, causing inflammation and damage. This interferes with the nerves' regular electrical impulse flow. There are four different types of MS: relapsing-remitting MS (RRMS) [15], secondary progressive MS (SPMS) [16], primary progressive MS (PPMS) [17], and progressive-relapsing MS (PRMS) [18]. The location and degree of CNS damage determine a wide range of symptoms associated with multiple sclerosis. Though its precise etiology is uncertain, MS is thought to result from synthesizing environmental and genetic variables. The goals of ongoing research are to increase our understanding of the fundamental causes of MS, create better therapies, and eventually find a cure. Improvements in neuroprotection, regenerative medicine, and immunotherapy may help prolong the lives of MS patients. In this study, I investigated the usability of ten 1,2-benzimidazole derivatives, which have not been synthesized before and are not available in the literature, in the treatment of MS disease by various theoretical calculations.

2. Methods

2.1. Studied Molecules

Ten different 1,2-benzimidazole derivative compounds (3-((6-(diethylamino)-2,3-dihydro-1H-inda zol-1-yl) methyl)-N,N-diethyl-1,2-dihydroquinolin-7-amine (1), 3-((6-(diethyl amino)-1H-benzo[d][1,2,3] triazol-1-yl) methyl)-N,N-diethyl-1,2-dihydroquinolin-7-amine (2), (7-(diethylamino)-1,2-dihydroquinolin-3-yl)(6-(diethylamino)-1H-benzo[d] [1,2,3]triazol-1-yl)methanol (3), (7-(diethylamino)-1,2-dihydro quinoline-3-yl)(6-(diethylamino)-1H-benzo[d] [1,2,3] triazol-1-yl) methanone (4), (7-(diethylamino)-1,2-dihydro-quinoline-3-yl)(6-(diethylamino)-2,3-dihydro-1H-indazol-1-yl)methanol (5), (7-(diethylamino)-1,2-di hydro-quinolin-3-yl)(6-(diethylamino)-2,3-dihydro-1H-indazol-1-yl)methanone (6), 3-(1-(6-(diethylamino)-2,3-dihydro-1H-indazol-1-yl)ethyl)-N,N-diethyl-1,2-di hydroquinolin-7-amine (7), 3-(1-(6-(diethylamino)-1H-benzo[d][1,2,3] triazol-1-yl)ethyl)-N,N-diethyl-1,2-dihydroquinolin-7-amine (8), 2-(7-(diethylamino)-1,2-dihydroquinolin-3-yl)-2-(6-(diethyl-amino)-2,3-dihydro-1H-indazol-1-yl) aceticacid (9), 2-(7-(diethylamino)-1,2-dihydroquinolin-3-yl)-2-(6-(diethyl amino)-1H-benzo[d][1,2,3] triazol-1-yl)aceticacid (10)) were selected for this study. The molecular formulas are given in Figure 1.
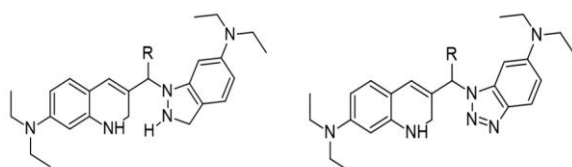
Molecule	-R
1	-H
5	-OH
6	=O
7	-CH₃
9	-COOH

Molecule	-R
2	-H
3	-OH
4	=O
8	-CH₃
10	-COOH

Fig. 1. Molecular formulas of the compounds used in the study.

2.2. Determination of the Target Protein

In this study, I first started with three drugs commonly used to treat MS to identify the target protein. The drugs I chose here are Ocrelizumab, Alemtuzumab, and Siponimod. Ocrelizumab is used in the treatment of Relapsing Forms of Multiple Sclerosis (RMS), RRMS, SPMS, and PPMS. The administration of Ocrelizumab involves intravenous (IV) infusion. Ocrelizumab is a monoclonal antibody that targets CD20-positive B cells. These white blood cells, or B cells, are a component of the immune system and are thought to be involved in the aberrant immunological response that causes myelin and nerve fiber destruction in multiple sclerosis. Ocrelizumab aids in lowering inflammation and slowing the disease's course by reducing these B cells [19]. Patients with relapsing types of MS are treated with a drug called Alemtuzumab. Patients who have not responded adequately to two or more previous MS medications are usually administered this medication. Alemtuzumab is given intravenously (IV) as a fusion. Alemtuzumab is a monoclonal antibody that specifically targets the CD52 protein, which is present on the surface of T and B lymphocytes, among other immune cells. Alemtuzumab kills these immune cells by attaching itself to CD52. This lessens inflammation and possible nerve fiber damage by lowering the aberrant immune response that targets the myelin sheath in MS patients [20]. Siponimod is a medication used to treat MS. Specifically, it is approved for the treatment of adult forms of Clinically Isolated Syndrome (CIS), RRMS, and SPMS. Siponimod is a modulator of the sphingosine 1-phosphate receptor. It functions by attaching itself to particular receptors on the surface of white blood cells called lymphocytes, which keep the lymphocytes inside the lymph nodes. This keeps the inflammation and damage that are typical of multiple sclerosis from being caused by these cells when they enter the central nervous system [21]. In this study, I analyzed the target proteins (3PP4, 6OBD, 7YXA, and 7TD4) with which these three drug-active ingredients interacted and examined their interactions with our 1,2-dihydroquinoline derivatives. All four target proteins I have chosen belong to the *Homo sapiens* organism. Images of the four different target proteins were obtained from the RCSB Protein Data Bank [22] and are given in Figure 2.
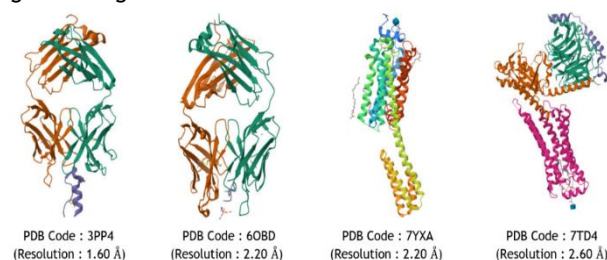

PDB Code : 3PP4 (Resolution : 1.60 Å)   PDB Code : 6OBD (Resolution : 2.20 Å)   PDB Code : 7YXA (Resolution : 2.20 Å)   PDB Code : 7TD4 (Resolution : 2.60 Å)

Fig. 2. Target proteins selected for molecular docking study.

2.3. Molecular Docking

In the molecular docking study of the identified target proteins and 1,2-dihydroquinoline derivatives molecules, I used the Auto Dock Vina 1.5.6 software tool, which I found to be widely used in the literature [23-27]. AutoDock Vina is a widely used software tool in the field of computational chemistry and bioinformatics for molecular docking studies at the same time a molecular docking software designed

to predict how small molecules, such as substrates or drug candidates, bind to a receptor of known 3D structure. Each ligand molecule was modified with hydrogen atoms and made polar before docking with the proteins. After optimizing our ligands, I performed docking with each ligand molecule and the selected proteins. In this docking study, the results were obtained for five different modes.

2.4. ADME Properties

I used the SwissADME [28] software program to determine the ADME properties of the 1,2-dihydroquinoline derivative molecules I examined in this study. SwissADME is an online program meant to estimate the pharmacokinetics, drug-likeness, and medicinal chemistry friendliness of compounds. It is commonly used in drug research and development to analyze the characteristics of potential drug candidates. In this study, BOILED-Egg graphic, bioavailability radar, physicochemical properties, lipophilicity, water solubility, pharmacokinetic properties, and pharmaceutical and medicinal chemistry properties were investigated for molecules of 1,2-dihydroquinoline derivatives. The BOILED-Egg graphic is a visual tool used in the SwissADME platform to predict and display the passive gastrointestinal absorption (HIA) and blood-brain barrier (BBB) properties of molecules. For oral bioavailability, the graphic aids in predicting a molecule's propensity to be passively absorbed in the gastrointestinal tract, and it calculates a molecule's ability to cross the BBB, a crucial factor for medications that aim to affect the central nervous system. The program plots the BOILED-Egg plot of molecules based on their predicted lipophilicity (WLOGP) and polarity (topological polar surface area, TPSA). Molecules falling within the white region are predicted to be passively absorbed by the gastrointestinal tract (high human intestinal absorption, HIA), and molecules falling within the yellow region are predicted to be able to penetrate the BBB [29]. A molecule's potential substrate status for P-glycoprotein (P-GP+: positive, color of blue; P-GP-: negative, color of red), a transporter protein that influences medication absorption and distribution, especially in the brain, can also be determined using the BOILED-Egg graphic. The BOILED-Egg graphic of the molecules I investigated is given in Figure 3.

Physicochemical properties are fundamental characteristics of molecules that influence their behavior in biological systems and their suitability as drug candidates. These characteristics are essential for the study of drug development, pharmacology, and medicinal chemistry. Physicochemical properties of each molecule: molecular weight (g/mol), number of heavy atoms, number of aromatic heavy atoms, fraction Csp^3, number of rotatable bonds, number of H-bond acceptors, number of H-bond donors, molar refractivity, and TPSA ($Å^2$) were calculated.

A visual tool used in drug development and discovery, the bioavailability radar allows researchers to rapidly determine a compound's bioavailability and drug likeness. By giving a graphical depiction of several important physicochemical characteristics, it enables researchers to quickly ascertain whether a molecule is within the ideal range for oral bioavailability. Bioavailability radar is based on six parameters [30]. These are: lipophilicity (LogP): measures the compound's hydrophobicity. Optimal range: -0.7 to +5.0. Size (MW) refers to the molecular weight of the compound. Optimal range: ≤500 Da. Polarity (TPSA, optimal range: 20-130 $Å^2$). Solubility (LogS) predicts aqueous solubility. Optimal range: not excessively insoluble (a broad range is often considered acceptable). Flexibility (number of rotatable bonds: affects the compound's conformational adaptability). Optimal range: ≤10. Saturation (Fraction Csp^3): indicates the degree of saturation. Optimal range: >0.25 [31]. Bioavailability radar plotted for molecules is given in Figure 4.
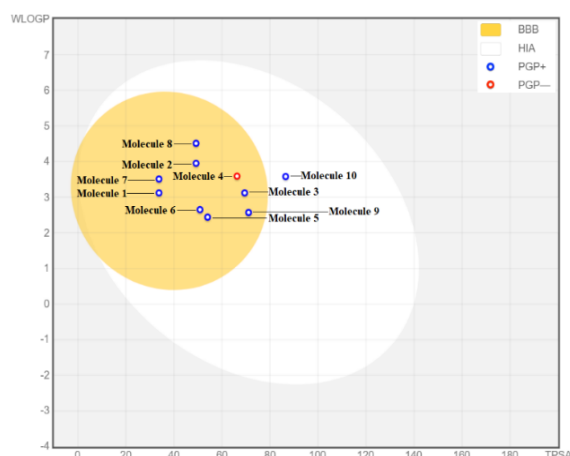

Fig. 3. The BOILED-Egg graphic of the molecules.

Molecule 1   Molecule 2   Molecule 3   Molecule 4   Molecule 5

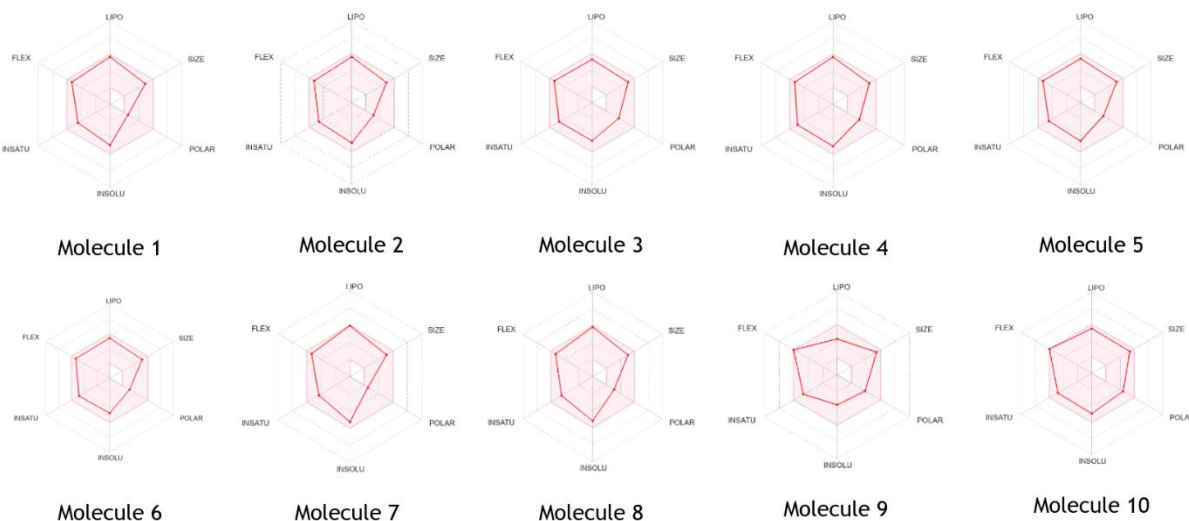Molecule 6   Molecule 7   Molecule 8   Molecule 9   Molecule 10

Fig. 4. Bioavailability radar graphic of the molecules.

In SwissADME, lipophilicity is a key parameter used to evaluate the drug-likeness and pharmacokinetic properties of molecules. It is typically expressed as the partition coefficient (logP), the partition coefficient between octanol and water, which measures how hydrophilic or hydrophobic a compound is. Consensus LogP: SwissADME provides a consensus logP value derived from multiple predictive models (XLOGP3, WLOGP, MLOGP, SILICOS-IT, and iLOGP). The octanol/water partition coefficient (logP) is a key measure of lipophilicity that plays a central role in this evaluation [32].

In SwissADME, water solubility is a key parameter used to evaluate the drug-likeness and pharmacokinetic properties of molecules. The term "water solubility" describes a compound's capacity to dissolve in water, which is essential for its distribution, absorption, and total bioavailability. SwissADME uses various computational methods to predict water solubility. These are ESOL (Estimated Solubility: uses fragment contributions and correction factors to estimate solubility), Ali's Solubility Model (a regression-based model that predicts solubility based on molecular properties), and SILICOS-IT (a method that combines molecular descriptors and machine learning algorithms to predict solubility). The logarithm of the compound's solubility in water is represented by the logS value. Better solubility is indicated by a greater logS. Solubility is divided into five different categories. These are in the form of very soluble (VS), soluble (S), moderately soluble (MS), poorly soluble (PS), and insoluble (IS). Drug-like substances typically fall into one of two ranges: 0 (very soluble) or -6 (poorly soluble) [33].

Pharmacokinetics in SwissADME involves the prediction and analysis of how a compound is ADME in the body. SwissADME offers instruments for assessing these characteristics, assisting researchers in identifying the drug-likeness and possible efficacy of compounds. As for pharmacokinetic properties, GI Absorption (prediction of gastrointestinal absorption to determine how well a compound can be absorbed when taken orally), and P-glycoprotein (P-gp) Substrate (determines if a compound is a substrate for P-glyco protein, a key transporter that can affect drug absorption and efflux) as absorption, BBB (important for drugs targeting the central nervous system), and Skin Permeation (logKp) (predicts the ability of a compound to permeate through the skin, useful for topical or transdermal drug delivery) as distribution, and Cytochrome P450 Interactions (predictions about whether a compound is a substrate, inhibitor, or inducer of major cytochrome P450 enzymes (CYP1A2, CYP2C19, CYP2C9, CYP2D6, CYP3A4), these enzymes play a crucial role in drug metabolism) as metabolism were examined [34].

Druglikeness in SwissADME refers to the qualitative assessment of a compound's potential to become an oral drug based on its chemical structure and properties. This idea facilitates the identification of substances with favorable pharmacokinetic and pharmacodynamic characteristics. SwissADME evaluates druglikeness using several criteria and rules, providing insights into the compound's suitability for drug development. At SwissADME, druglikeness is evaluated according to five rules. These are Lipinski (molecular weight less than 500 Daltons, LogP (octanol-water partition coefficient) less than 5, the number of hydrogen bond donors less than 5, and the number of hydrogen bond acceptors less than 10. These rules help predict oral bioavailability, and compounds that violate more than one of these rules are less likely to be orally active drugs), Ghose (molecular weight between 160 and 480 Daltons, LogP between -0.4 and 5.6, molar refractivity between 40 and 130, total number of atoms between 20 and 70; this filter helps refine druglikeness by adding constraints on molecular size and complexity), Veber (number of rotatable bonds less than 10 and Polar Surface Area (PSA) less than 140 $Å^2$; these rules emphasize molecular flexibility and surface area, which influence oral bioavailability and permeability), Egan (LogP between -1 and 5, PSA less than 131 $Å^2$; this rule set is another refinement focusing on the balance of hydrophobicity and polarity), and Muegge (LogP between -2 and 5, number of hydrogen bond donors less than 5, number of hydrogen bond acceptors less than 10, molecular weight between 200 and 600 Daltons, number of rings less than 7; this filter adds additional constraints to focus on the most drug-like molecules). In addition, the Bioavailability Score (which provides a score based on compliance with multiple druglikeness rules, indicating the overall likelihood of oral bioavailability) calculation is also made in this context [35].

PAINS (Pan Assay Interference Compounds), Brenk, Leadlikeness, and synthetic accessibility values were calculated as medicinal chemistry in SwissADME. In SwissADME, PAINS filters are used in medicinal chemistry to identify and exclude compounds that are likely to give false-positive results in high-throughput screening (HTS) assays. These substances have the ability to obstruct a variety of test types by aggregating proteins, reacting in an unintended way, or fluorescing. PAINS are compounds that frequently show activity in multiple assay types due to their interference properties rather than specific binding to a target [36]. In SwissADME, the numbers, such as 0, 1, 2, etc., given in the PAINS section indicate the count of PAINS alerts triggered by the compound being analyzed. Each alert corresponds to the presence of a structural motif known to cause assay interference. In SwissADME, the Brenk filter is used to identify potentially problematic substructures within a molecule that are considered undesirable in drug discovery. These substructures, which are sometimes called structural alerts or toxicophores, might cause toxicity, poor pharmacokinetic characteristics, or interference with assays, among other problems [37]. Leadlikeness is a term used in SwissADME to assess if a molecule has qualities that would make it a good place to start (or lead) for drug development. At SwissADME, leadlikeness is evaluated according to five different criteria. These are molecular weights (typically between 250 and 350 Daltons). Smaller molecular weight compounds are preferred because they can be modified more easily during the optimization process. LogP (octanol-water partition coefficient) is generally between 1 and 3. This range indicates moderate lipophilicity, balancing solubility and permeability, and the number of hydrogen bond donors (preferably less than 3). Lower numbers help ensure good membrane permeability and oral bioavailability, and the number of hydrogen bond acceptors (preferably less than 6). Similar to hydrogen bond donors, this helps with membrane permeability and bioavailability. The number of rotatable bonds is preferably less than 8. Fewer rotatable bonds typically lead to better conformational stability and favorable pharmacokinetic properties [38].

Finally, Synthetic Accessibility Score (SAscore) was calculated specifically for medicinal chemistry. Synthetic accessibility in SwissADME refers to the ease with which a compound can be synthesized. This idea is crucial to medicinal chemistry since, in order to be taken seriously as a promising drug candidate, a molecule must be practically synthesized in addition to having desirable biological activity and drug-like qualities. SAscore ranges from 1 to 10 (1: indicates very easy to synthesize, 10: indicates very difficult to synthesize).

2.5. Bioactivity Score

An online cheminformatics platform called Molinspiration offers tools for calculating molecular characteristics, predicting bioactivity, analyzing drug-likeness, and other significant pharmacokinetic aspects. In medicinal chemistry and drug discovery, these instruments are frequently employed by researchers to assess and refine possible therapeutic options. Molinspiration can predict the bioactivity of compounds across various target classes, such as GPCR ligands, ion channel modulators, kinase inhibitors, nuclear receptor ligands, protease inhibitors, and enzyme inhibitors. This helps in identifying potential biological activities early in the drug discovery process [39].

2.6. Toxicity Risks and Drug Scores

An online program called OSIRIS Property Explorer is used in medicinal chemistry to anticipate different chemical properties and assess possible therapeutic candidates. Early on in the drug development process, it helps researchers make well-informed judgments by offering insights regarding toxicity risks, drug-likeness, and overall drug scores [40]. Toxicity risks (mutagenic, tumorigenic, irritant, and reproductive effective), drug-likeness score, and drug-score were calculated for all molecules considered in this study. I also used TEST (Toxicity Estimation Software Tool). The U.S. Environmental

Protection Agency (EPA) created TEST, a software program intended to forecast different toxicological and environmental characteristics of chemical compounds. Based on a compound's molecular structure, TEST estimates a compound's toxicity and physical characteristics using quantitative structure-activity relationship (QSAR) models [41]. Using this program, fathead minnow LC_{50} (96 hr), *Daphnia magna* LC_{50} (48 hr), oral rat LD_{50}, bioconcentration factor (which indicates the potential of a substance to accumulate in living organisms), and density are calculated for each molecule.

2.7. Quantum Mechanical Parameters

In molecular modeling and computational chemistry, quantum mechanical parameters are essential. At the quantum level, they explain a variety of molecular characteristics and behaviors [42]. The Schrödinger equation for molecular systems is solved using quantum mechanical computations, from which these values are obtained. First, E_{HOMO} and E_{LUMO} values were calculated according to DFT methods on the basis set of B3LYP 6-311+G(2d,p) with the Gaussian 09W program. With the help of these calculated values of E_{HOMO} and E_{LUMO}, chemical potential (μ), electron affinity (EA), global softness (S), global hardness (η), ionization potential (IP), and electrophilicity were calculated. The self-consistent field (SCF) energy (Hartree) and dipole moment (Debye) values of each molecule were also calculated with the help of the same computer program.

3. Results

The data I obtained as a result of the docking study between our molecules and the proteins (3PP4, 6OBD, 7YXA, and 7TD4-coded proteins) I identified using the Auto Dock Vina software tool are given in Table 1.

Table 1. The obtained molecular docking results.

Molecule	Protein (PDB Code)	Affinity (kcal/mol)				
		Mode 1	Mode 2	Mode 3	Mode 4	Mode 5
1	3PP4	-8.00	-7.00	-7.00	-6.70	-6.30
	6OBD	-8.30	-8.20	-7.70	-6.60	-6.50
	7YXA	-9.00	-8.80	-8.40	-7.70	-7.30
	7TD4	-10.00	-9.00	-7.40	-7.00	-6.90
2	3PP4	-7.90	-7.30	-7.00	-6.40	-6.20
	6OBD	-8.20	-8.10	-7.70	-7.10	-6.60
	7YXA	-8.70	-8.60	-8.30	-7.30	-7.10
	7TD4	-10.30	-8.60	-7.40	-7.00	-7.00
3	3PP4	-8.00	-7.50	-7.10	-7.10	-6.20
	6OBD	-8.50	-8.40	-8.10	-7.20	-7.00
	7YXA	-8.90	-8.70	-8.40	-7.50	-7.50
	7TD4	-10.10	-8.90	-7.30	-7.00	-6.90
4	3PP4	-8.40	-7.30	-6.70	-6.30	-6.30
	6OBD	-8.50	-8.00	-7.50	-6.70	-6.60
	7YXA	-8.30	-8.30	-7.10	-7.10	-6.50
	7TD4	-10.60	-9.20	-7.40	-7.40	-7.20
5	3PP4	-8.10	-7.30	-7.10	-6.80	-6.70
	6OBD	-8.70	-8.40	-8.20	-7.30	-6.80
	7YXA	-9.00	-8.90	-8.70	-7.70	-7.20
	7TD4	-10.20	-9.60	-7.50	-7.30	-7.00

	3PP4	-8.50	-7.90	-6.60	-6.40	-6.20
6	6OBD	-8.80	-7.80	-7.70	-6.80	-6.70
	7YXA	-9.60	-8.60	-8.40	-7.70	-7.00
	7TD4	-10.60	-9.10	-7.70	-7.60	-7.40
	3PP4	-7.80	-6.70	-6.60	-6.50	-5.90
7	6OBD	-8.00	-8.00	-6.60	-6.60	-6.30
	7YXA	-9.40	-8.90	-8.30	-8.00	-7.10
	7TD4	-8.80	-8.50	-7.40	-7.30	-7.30
	3PP4	-8.20	-6.90	-6.90	-6.60	-6.10
8	6OBD	-8.20	-8.10	-6.90	-6.80	-6.40
	7YXA	-9.00	-8.90	-8.70	-7.60	-7.30
	7TD4	-9.70	-9.10	-7.40	-7.40	-7.30
	3PP4	-8.30	-7.20	-6.90	-6.70	-6.70
9	6OBD	-8.30	-8.00	-7.20	-6.80	-6.60
	7YXA	-8.50	-8.40	-7.90	-7.30	-6.80
	7TD4	-9.00	-8.90	-7.90	-7.50	-7.20
	3PP4	-8.40	-7.60	-7.00	-6.90	-6.80
10	6OBD	-8.60	-8.10	-6.90	-6.80	-6.70
	7YXA	-8.80	-8.80	-8.60	-7.10	-6.70
	7TD4	-10.00	-9.30	-7.60	-7.30	-7.30

When the data in Table 1 are analyzed, it is seen that the highest docking score was obtained for the (7 (diethylamino)-1,2-dihydroquinolin-3-yl)(6-(diethylamino) - 2,3-dihydro-1H-indazol-1-yl) methanone (molecule 6) with our four proteins. When I examined the interactions of molecule number six with four proteins (3PP4, 6OBD, 7YXA, and 7TD4), it was observed that there were van der Waals, hydrogen bond, carbon hydrogen bond, alkyl, and pi-alkyl interactions between our molecule and the protein coded 3PP4. As a result of these interactions, a docking score of -8.5 kcal/mol was obtained. 2D and 3D images of these interactions are given in Figures 5 and 6.
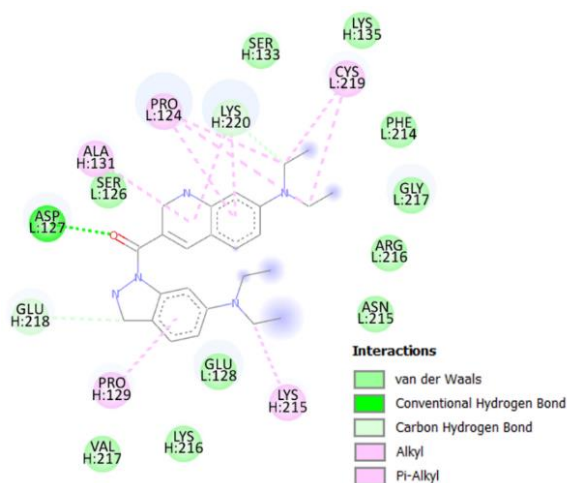

Fig. 6. 3D image of the interaction between the 3PP4 coded protein with molecule number 6.

interactions are given in Figures 7 and 8. It was observed that there were van der Waals, hydrogen bond, carbon hydrogen bond, pi-pi stacked, alkyl, and pi-alkyl interactions between molecule number six and the protein coded 7YXA. As a result of these interactions, a doking score of -9.6 kcal/mol was obtained. 2D and 3D images of these interactions are given in Figures 9 and 10.

Fig. 5. 2D image of the interaction between the 3PP4 coded protein with molecule number 6.

It was observed that there were van der Waals, hydrogen bond, carbon hydrogen bond, pi-donor hydrogen bond, pi-pi T-shaped, and pi-alkyl interactions between molecule number six and the protein coded 6OBD. As a result of these interactions, a docking score of -8.8 kcal/mol was obtained. 2D and 3D images of these
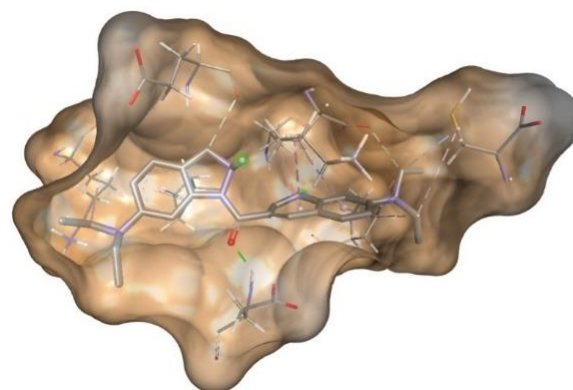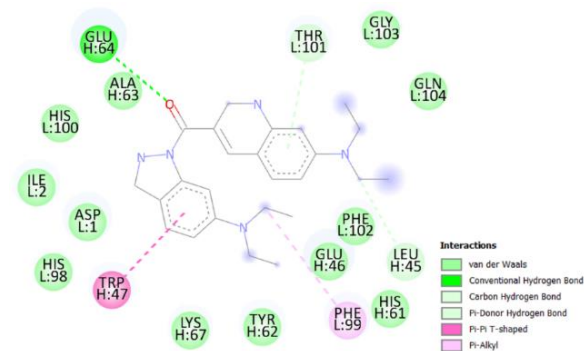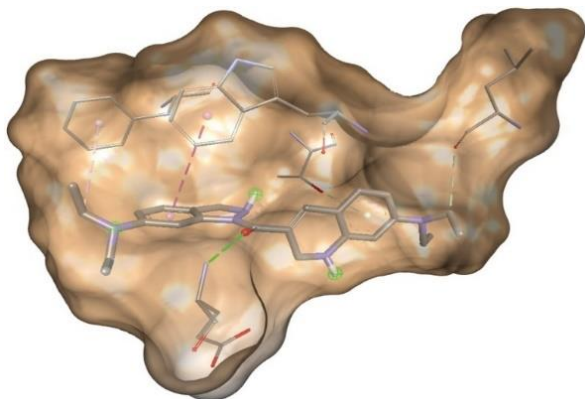

Fig. 7. 2D image of the interaction between the 6OBD coded protein with molecule number 6.

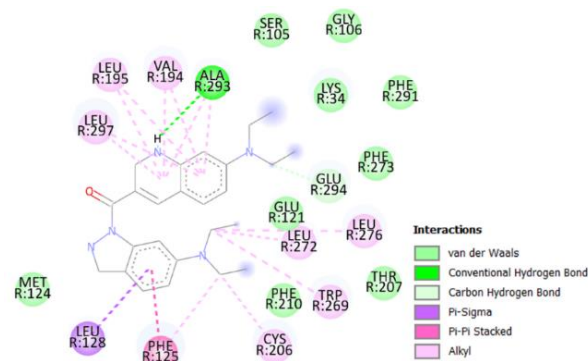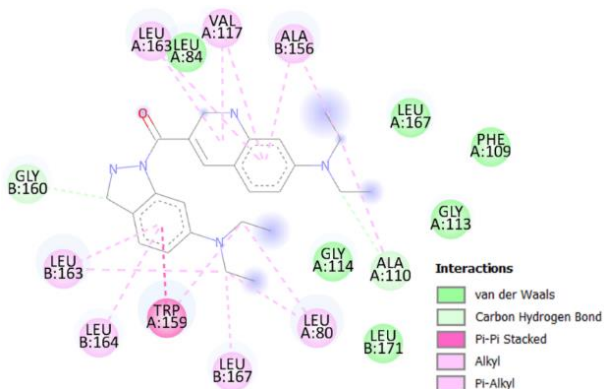**Fig. 8.** 3D image of the interaction between the 6OBD coded protein with molecule number 6.

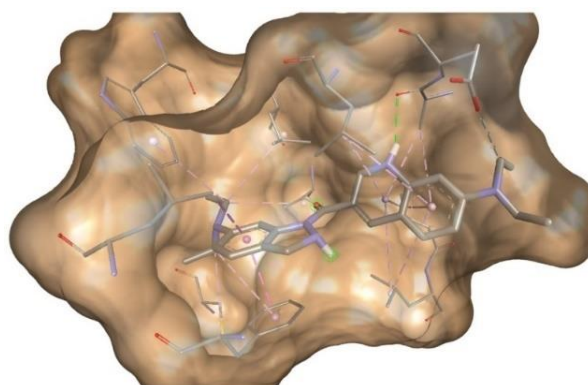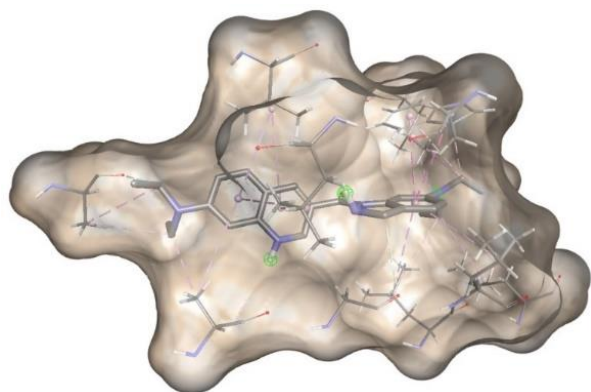**Fig. 9.** 2D image of the interaction between the 7YXA coded protein with molecule number 6.

Fig. 10. 3D image of the interaction between the 7YXA coded protein with molecule number 6.

Finally, it was observed that there were van der Waals, hydrogen bond, carbon hydrogen bond, pi-sigma, pi-pi stacked, and alkyl interactions between molecule number six and the protein coded 7TD4. As a result of these interactions, a doking score of -10.6 kcal/mol was obtained. The best interaction and docking score were obtained as a result of the interaction with this 7TD4 protein. 2D and 3D images of these interactions are given in Figures 11 and 12.

Fig. 11. 2D image of the interaction between the 7TD4 coded protein with molecule number 6.

Fig. 12. 3D image of the interaction between the 7TD4 coded protein with molecule number 6.
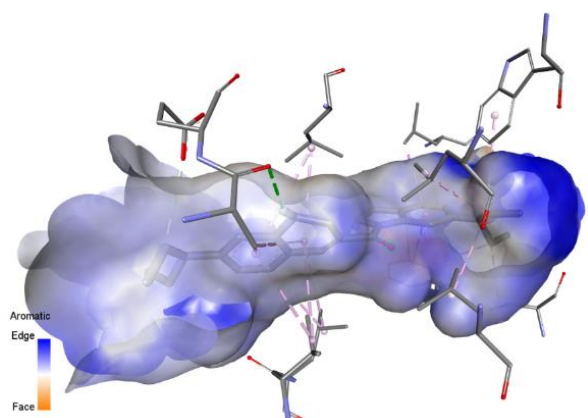

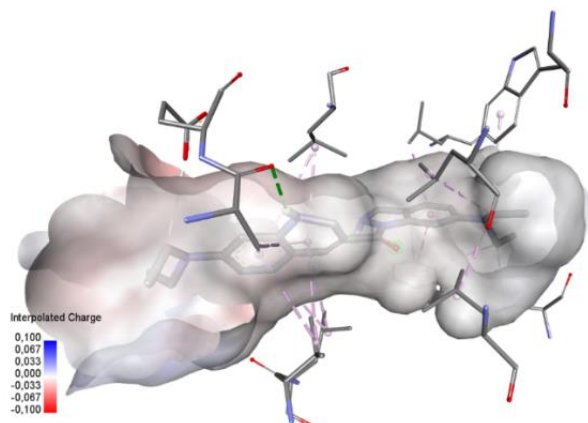**Fig. 13.** Three-dimensional aromatic structures of molecule number 6.

Fig. 14. Three-dimensional interpolated charge structures of molecule number 6.
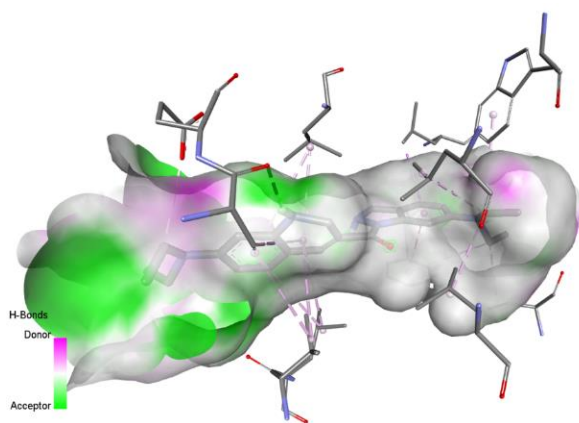
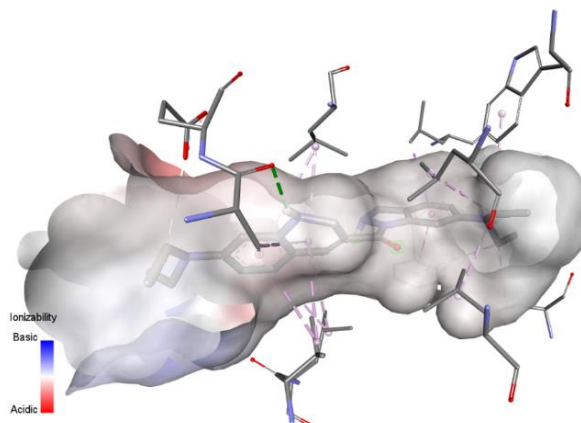**Fig. 15.** Three-dimensional H-bonds structures of molecule number 6.

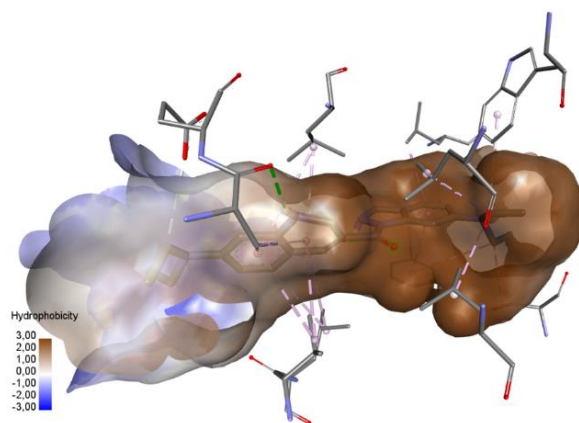**Fig. 17.** Three-dimensional ionizability structures of molecule number 6.

Fig. 16. Three-dimensional hydrophobicity structures of molecule number 6.
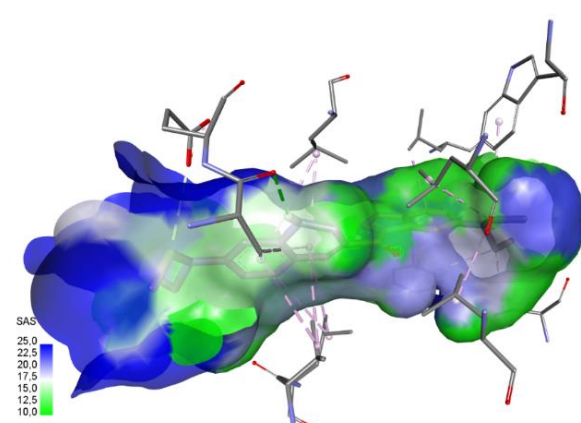

Fig. 18. Three-dimensional SAS (solvent accessible surface area) structures of molecule number 6.

Since I have identified the most ideal molecule 6, I will interpret all other results for this molecule. When I examine the BOILED-Egg graphic of the molecules given in Figure 3, it is seen that molecule 6 can cross the blood-brain barrier. This is a very important feature for MS treatment. When the bioavailability radar graphic of the molecules in Figure 4 is analyzed, it is seen that molecule 6 complies with all six parameters (lipophilicity, size, polarity, solubility, saturation, and flexibility), and the red line is located in the pink area. This shows us that the molecule can be considered an ideal active drug ingredient.

Firstly, physicochemical properties were calculated for each molecule. These related data are given in Table 2. Then, the lipophilicity values I calculated are given in Table 3. When I examined the data given in Table 3 to evaluate molecule 6 in terms of lipophilicity, it was obtained that the lipophilicity values for Log $P_{O/W}$ (iLOGP), Log $P_{O/W}$ (XLOGP3), Log $P_{O/W}$ (WLOGP), Log $P_{O/W}$ (MLOGP), Log $P_{O/W}$ (SILICOS-IT), and consensus Log $P_{O/W}$ were between -0.7 and +5.0. This means that the molecule is ideal in terms of lipophilicity.

Table 2. Physicochemical properties of molecules.

Molecule	Formula	Physicochemical properties								
		Molecular weight (g/mol)	Number of heavy atoms	Number of aromatic heavy atoms	Fraction Csp^3	Number of rotatable bonds	Number of H-bond acceptors	Number of H-bond donors	Molar Refractiv.	TPSA (Å^2)
1	$C_{25}H_{35}N_5$	405.58	30	12	0.44	8	1	2	140.53	33.78
2	$C_{24}H_{32}N_6$	404.55	30	15	0.42	8	2	1	130.98	49.22
3	$C_{24}H_{32}N_6O$	420.55	31	15	0.42	8	3	2	132.14	69.45
4	$C_{24}H_{30}N_6O$	418.53	31	15	0.38	8	3	1	131.40	66.29
5	$C_{25}H_{35}N_5O$	421.58	31	12	0.44	8	2	3	141.70	54.01
6	$C_{25}H_{33}N_5O$	419.56	31	12	0.40	8	2	2	140.73	50.85
7	$C_{26}H_{37}N_5$	419.61	31	12	0.46	8	1	2	145.34	33.78
8	$C_{25}H_{34}N_6$	418.58	31	15	0.44	8	2	1	135.78	49.22
9	$C_{26}H_{35}N_5O_2$	449.59	33	12	0.42	9	3	3	147.11	71.08
10	$C_{25}H_{32}N_6O_2$	448.56	33	15	0.40	9	4	2	137.56	86.52

Table 3. Lipophilicity values of molecules.

Lipophilicity	Molecule									
	1	2	3	4	5	6	7	8	9	10
Log $P_{O/w}$ (iLOGP)	4.14	3.59	3.44	4.06	1.48	4.18	3.99	4.00	3.35	3.21
Log $P_{O/w}$ (XLOGP3)	4.48	4.32	3.77	4.43	3.93	4.05	4.89	4.72	2.00	4.11
Log $P_{O/w}$ (WLOGP)	3.12	3.95	3.12	3.59	2.44	2.65	3.51	4.51	2.57	3.58
Log $P_{O/w}$ (MLOGP)	3.79	3.69	3.30	3.63	3.38	3.30	3.99	3.90	3.11	3.05
Log $P_{O/w}$ (SILICOS-IT)	3.42	3.13	2.35	2.68	2.64	2.97	3.65	3.36	2.60	2.31
Consensus Log $P_{O/w}$	3.79	3.74	3.20	3.68	2.77	3.43	4.00	4.10	2.73	3.25

When I examine the lipophilicity values, the fact that all values are within the desired range shows that I can evaluate each of them positively in terms of lipophilicity. When I examined the data given in Table 4 to evaluate the molecule 6 in terms of water solubility, it was obtained that the water solubility value for ESOL, Ali, and SILICOS-IT was between -4.75 and -6.90. This tells us that the molecule is moderately soluble for ESOL and Ali and poorly soluble for SILICOS-IT in terms of water solubility. Based on these results, I can say that it is moderately soluble on average.

It was determined that GI absorption was high for Molecule 6 and P-glycoprotein (P-gp) substrate was positive when I examined the pharmacokinetics properties values given in Table 5. In terms of distribution, BBB is positive, and logKp is -5.98 cm/s. Finally, in terms of metabolism, cytochrome P450 interactions are positive for CYP2C19 and CYP2D6 and negative for CYP1A2, CYP2C9, and CYP3A4.

It is determined that all molecules, such as molecule 6, have druglikeness properties according to Lipinski, Veber, Egan, and Muegge, but according to Ghose, it does not have druglikeness properties because the molar refractivity is > 130 when I examine the data given in Table 6 in terms of druglikeness properties. A molecule's ability to be polarized is indicated by its molar refractivity. It is defined as the volume, corrected for refractive index, that one mole of a substance occupies. A bioavailability score is a score based on compliance with multiple drug compliance rules. The bioavailability score of 0.55 for molecule 6 is also very positive for us.

Table 4. Water solubility values of molecules.

Molecule	ESOL				Ali				SILICOS-IT			
	Log S	Solubility (mg/mL)	Solubility (mol/L)	Class*	Log S	Solubility (mg/mL)	Solubility (mol/L)	Class*	Log S	Solubility (mg/mL)	Solubility (mol/L)	Class*
1	-4.94	4.60E-03	1.14E-05	MS	-4.91	5.00E-03	1.23E-05	MS	-7.37	1.73E-05	4.27E-08	PS
2	-4.91	4.96E-03	1.23E-05	MS	-5.07	3.46E-03	8.56E-06	MS	-7.03	3.80E-05	9.40E-08	PS
3	-4.65	9.36E-03	2.23E-05	MS	-4.92	5.04E-03	1.20E-05	MS	-6.08	3.49E-04	8.30E-07	PS
4	-5.06	3.68E-03	8.79E-06	MS	-5.54	1.21E-03	2.88E-06	MS	-6.56	1.16E-04	2.77E-07	PS
5	-4.69	8.64E-03	2.05E-05	MS	-4.76	7.27E-03	1.72E-05	MS	-6.42	1.59E-04	3.77E-07	PS
6	-4.75	7.44E-03	1.77E-05	MS	-4.82	6.33E-03	1.51E-05	MS	-6.90	5.27E-05	1.26E-07	PS
7	-5.28	2.20E-03	5.24E-06	MS	-5.33	1.94E-03	4.62E-06	MS	-7.39	1.72E-05	4.09E-08	PS
8	-5.24	2.42E-03	5.77E-06	MS	-5.48	1.38E-03	3.29E-06	MS	-7.04	3.77E-05	9.02E-08	PS
9	-3.56	1.23E-01	2.74E-04	S	-3.12	3.42E-01	7.60E-04	S	-6.35	2.03E-04	4.51E-07	PS
10	-4.95	5.00E-03	1.11E-05	MS	-5.63	1.04E-03	2.33E-06	MS	-6.00	4.45E-04	9.93E-07	PS

(*; S : Soluble, MS : Moderately soluble, PS : Poorly soluble)

Table 5. Pharmacokinetics properties of molecules.

Molecule	Pharmacokinetics Properties								
	Absorption		Distribution		Metabolism				
	GI Absorption	P-glycoprotein (P-gp) Substrate	Blood-Brain Barrier (BBB) Permeation	Skin Permeation (logKp,cm/s)	Cytochrome P450 Interactions				
					CYP 1A2	CYP 2C19	CYP 2C9	CYP 2D6	CYP 3A4
1	High	Yes	Yes	-5.59	No	Yes	No	Yes	No
2	High	Yes	Yes	-5.70	No	Yes	Yes	Yes	Yes
3	High	Yes	Yes	-6.19	No	No	Yes	Yes	Yes
4	High	No	Yes	-5.71	No	Yes	Yes	Yes	Yes
5	High	Yes	Yes	-6.08	No	No	No	Yes	Yes
6	High	Yes	Yes	-5.98	No	Yes	No	Yes	No
7	High	Yes	Yes	-5.39	No	Yes	No	Yes	Yes
8	High	Yes	Yes	-5.50	No	No	Yes	Yes	Yes
9	High	Yes	Yes	-7.62	No	No	No	Yes	No
10	High	Yes	No	-6.12	No	Yes	Yes	Yes	Yes

Table 6. Druglikeness properties of molecules

Molecule	Druglikeness Properties					
	Lipinski	Ghose	Veber	Egan	Muegge	Bioavailability Score
1	Yes	No, MR>130	Yes	Yes	Yes	0.55
2	Yes	No, MR>130	Yes	Yes	Yes	0.55
3	Yes	No, MR>130	Yes	Yes	Yes	0.55
4	Yes	No, MR>130	Yes	Yes	Yes	0.55
5	Yes	No, MR>130	Yes	Yes	Yes	0.55
6	Yes	No, MR>130	Yes	Yes	Yes	0.55
7	Yes	No, MR>130	Yes	Yes	Yes	0.55
8	Yes	No, MR>130	Yes	Yes	Yes	0.55
9	Yes	No, MR>130	Yes	Yes	Yes	0.85
10	Yes	No, MR>130	Yes	Yes	Yes	0.56

I analyzed the data given in Table 7 in terms of medicinal chemistry properties. The PAINS value of 2 for molecule 6 is important as it indicates the number of PAINS alerts triggered by the analyzed compound, as given in the PAINS section. The Brenk filter is used to identify potentially problematic substructures within a molecule that are considered undesirable in drug discovery, and setting this value to 0 for molecule 6 was also perceived as a positive result. It was concluded that none of the other molecules, such as molecule 6, carried the leadlikeness property. Especially for molecule 6, the fact that it was MW > 350, Rotors > 7, and XLOGP3 > 3.5 caused it not to have this feature. The synthetic accessibility score ranges from 1 to 10 (1 indicates very easy synthesizing, 10 indicates very difficult synthesizing). I get an order of 4>2>6>1>3> 5>=8>10>7>9 when I rank the molecules in order of ease of synthesis. Here I see that molecule 6 can be synthesized easily.

Table 7. Medicinal chemistry properties of molecules.

Molecule	Medicinal Chemistry Properties			
	PAINS	Brenk	Leadlikeness	Synthetic Accessibility Score (SAscore)
1	2	0	No, MW > 350 Rotors > 7; XLOGP3 > 3.5	4.23
2	1	0	No, MW > 350 Rotors > 7; XLOGP3 > 3.5	4.15
3	1	0	No, MW > 350 Rotors > 7; XLOGP3 > 3.5	4.71
4	1	0	No, MW > 350 Rotors > 7; XLOGP3 > 3.5	4.09
5	2	0	No, MW > 350 Rotors > 7; XLOGP3 > 3.5	4.76
6	2	0	No, MW > 350 Rotors > 7; XLOGP3 > 3.5	4.18
7	2	0	No, MW > 350 Rotors > 7; XLOGP3 > 3.5	4.86
8	1	0	No, MW > 350 Rotors > 7; XLOGP3 > 3.5	4.76
9	2	0	No, MW > 350 Rotors > 7	4.90
10	1	0	No, MW > 350 Rotors > 7; XLOGP3 > 3.5	4.80

Table 8. Bioactivity Scores of molecules.

Molecule	Bioactivity Score*					
	GPCR ligand	Ion channel modulator	Kinase inhibitor	Nuclear receptor ligand	Protease inhibitor	Enzyme inhibitor
1	-0.07	-0.20	-0.14	-0.14	-0.21	-0.10
2	-0.04	-0.36	-0.11	-0.17	-0.31	-0.14
3	-0.01	-0.26	-0.07	-0.23	-0.25	-0.06
4	-0.08	-0.47	-0.11	-0.24	-0.38	-0.18
5	-0.01	-0.17	-0.10	-0.07	-0.09	-0.03

6	-0.07	-0.22	-0.16	-0.15	-0.14	-0.10
7	-0.03	-0.17	-0.12	-0.13	-0.16	-0.08
8	-0.06	-0.35	-0.07	-0.26	-0.41	-0.21
9	0.04	-0.11	-0.17	-0.01	-0.05	0.01
10	-0.01	-0.34	-0.17	-0.10	-0.26	-0.13

(*: low bioactivity: -10 to -5, moderate bioactivity: -5 to 0, high bioactivity: 0 to 5, very high bioactivity: 5 to 10)

A high bioactivity score indicates a strong and effective biological interaction, which is promising for drug development, while a low bioactivity score suggests a need for further optimization or alternative approaches. It is observed that the data are generally between 0 and -0.5 when the data in Table 8 is examined. For molecule 6, the values are seen to be between -0.07 and -0.22. This shows us that molecule 6 has moderate bioactivity.
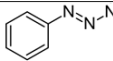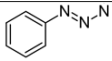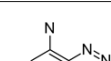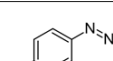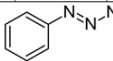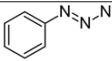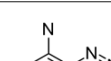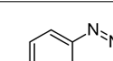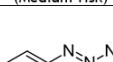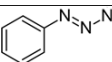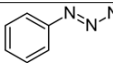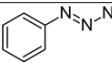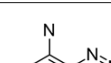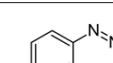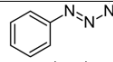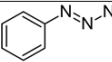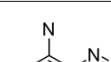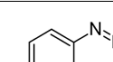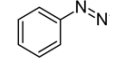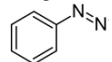
It is seen that molecule 6 has none of the mutagenic, tumorigenic, irritant, or reproductively effective properties in terms of toxicity risks when the data in Table 9, where toxicity risks, drug-likeness scores, and drug-scores are given for all molecules, are examined. This shows us that this molecule is the most ideal molecule in terms of usability as a drug-active ingredient. In drug discovery and development, the drug-likeness score is a metric used to assess if a chemical compound has the necessary qualities to be developed into a drug. This score evaluates how well the compound's physical and chemical characteristics, which are linked to advantageous

pharmacokinetics and pharmacodynamics, resemble those of well-known medications. Molecule 6 has the highest drug-likeness score (5.40) among all molecules. Likewise, drug scores (0.68) are also a good score.

Fathead minnow LC_{50} (96 hr), D*aphnia magna* LC_{50} (48 hr), and oral rat LD_{50} values of the molecules are presented in Table 10. The bioconcentration factor is a critical parameter in ecotoxicology, providing insights into the potential for substances to accumulate in aquatic organisms and the broader environmental implications of chemical pollutants. Molecule 6 appears to have low bioconcentration potential.

The density of a drug refers to its mass per unit volume, just like the density of any other material. It is an important physical property in the pharmaceutical sciences and has implications for the formulation, manufacturing, and administration of drugs. The value of 1.19 g/cm^3 obtained for molecule 6 is considered to be a very ideal value for us.

Table 9. Toxicity risks and drug-scores for molecules.

Using the Gaussian 09W program, the E_{HOMO} and E_{LUMO} values were determined using DFT methods on the basis set of B3LYP 6-311+G(2d,p). Figure 19 provides a visual representation of the E_{HOMO} and E_{LUMO} values. Chemical potential (μ), electron affinity (EA), global softness (S), global hardness (η), ionization potential (IP), and electrophilicity were all determined with the aid of these computed values of E_{HOMO} and E_{LUMO}. Table 11 provides the obtained values. SCF energy (Hartree) and dipole moment values (Debye) are given in Table 12. These values was calculated to obtain more information about the molecules.

Table 10. Fathead minnow LC_{50} (96 hr), daphnia magna LC_{50} (48 hr), oral rat LD_{50}, bioconcentration factor, and density values of molecules.

Molecule	Fathead minnow LC_{50} (96 hr)		Daphnia magna LC_{50} (48 hr)		Oral rat LD_{50}		Bioconcentration factor	Density (g/cm³)
	-log10 (mol/L)	mg/L	-log10 (mol/L)	Density (g/cm³)	-log10 (mol/kg)	mg/kg		
1	6.19	0.26	5.19	2.60	2.77	687.29	26.20	1.14
2	6.47	0.14	5.39	1.66	2.80	644.26	40.84	1.23
3	6.66	9.28E-02	5.08	3.53	2.78	695.89	24.79	1.27
4	6.77	7.16E-02	5.23	2.48	2.78	696.22	18.71	1.27
5	6.24	0.24	5.07	3.61	2.76	732.06	21.38	1.19
6	6.27	0.22	5.02	4.03	2.79	684.67	15.47	1.19
7	6.32	0.22	5.30	2.08	2.78	696.07	56.25	1.12
8	6.78	6.88E-02	5.52	1.28	2.78	696.10	50.52	1.22
9	6.62	0.11	4.78	7.42	2.80	707.73	3.40	1.24
10	7.03	4.17E-02	4.45	15.86	2.85	635.15	5.02	1.33
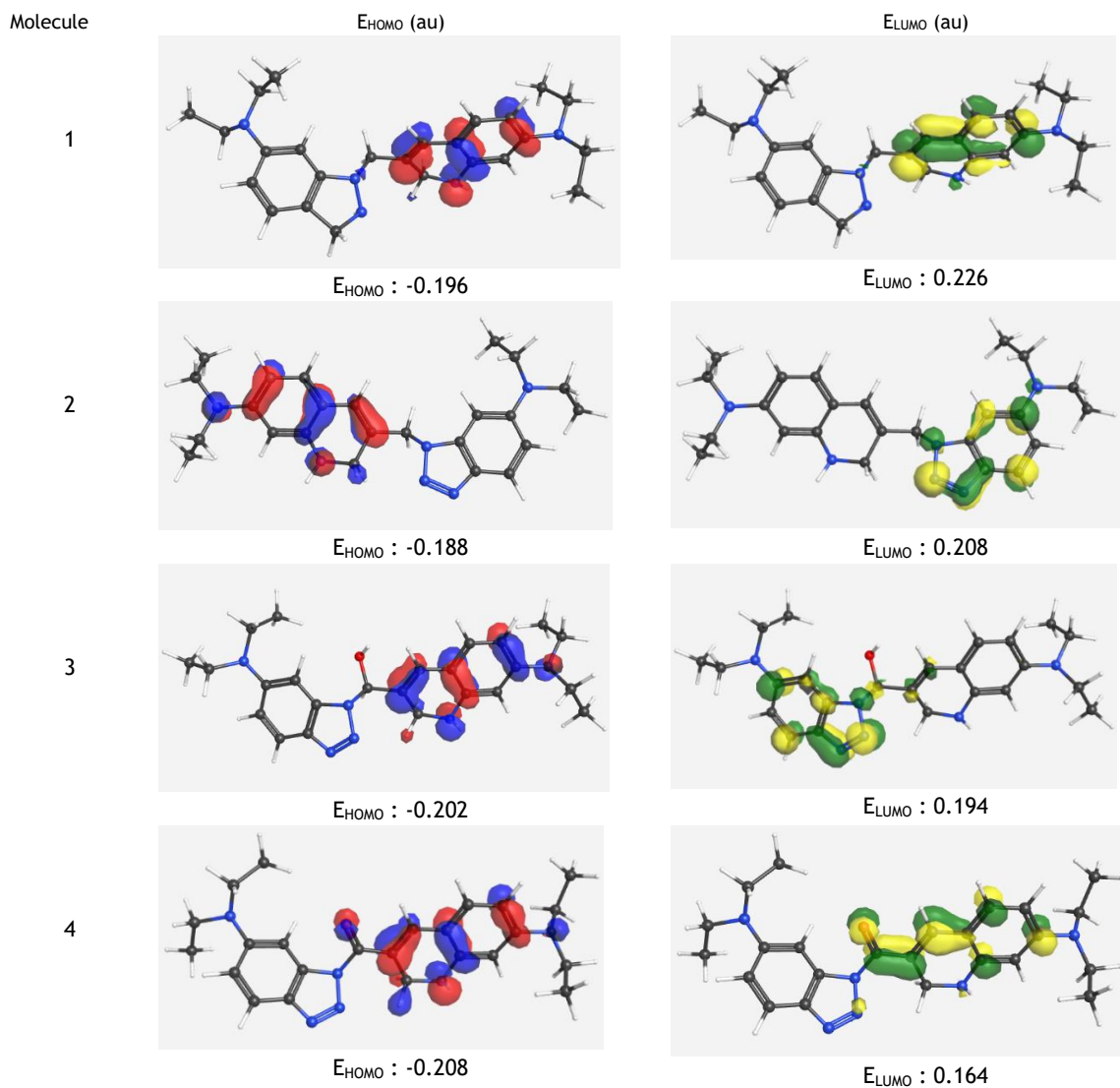
Molecule	E_{HOMO} (au)	E_{LUMO} (au)

1

E_{HOMO} : -0.196

E_{LUMO} : 0.226

2

E_{HOMO} : -0.188

E_{LUMO} : 0.208

3

E_{HOMO} : -0.202

E_{LUMO} : 0.194

4

E_{HOMO} : -0.208

E_{LUMO} : 0.164

Fig. 19. Visual representation of E_{HOMO} and E_{LUMO} values for all molecules.

5

E_{HOMO} : -0.189 E_{LUMO} : 0.227

6

E_{HOMO} : -0.194 E_{LUMO} : 0.191

7

E_{HOMO} : -0.189 E_{LUMO} : 0.229

8

E_{HOMO} : -0.199 E_{LUMO} : 0.201

9

E_{HOMO} : -0.200 E_{LUMO} : 0.218

10

E_{HOMO} : -0.210 E_{LUMO} : 0.191
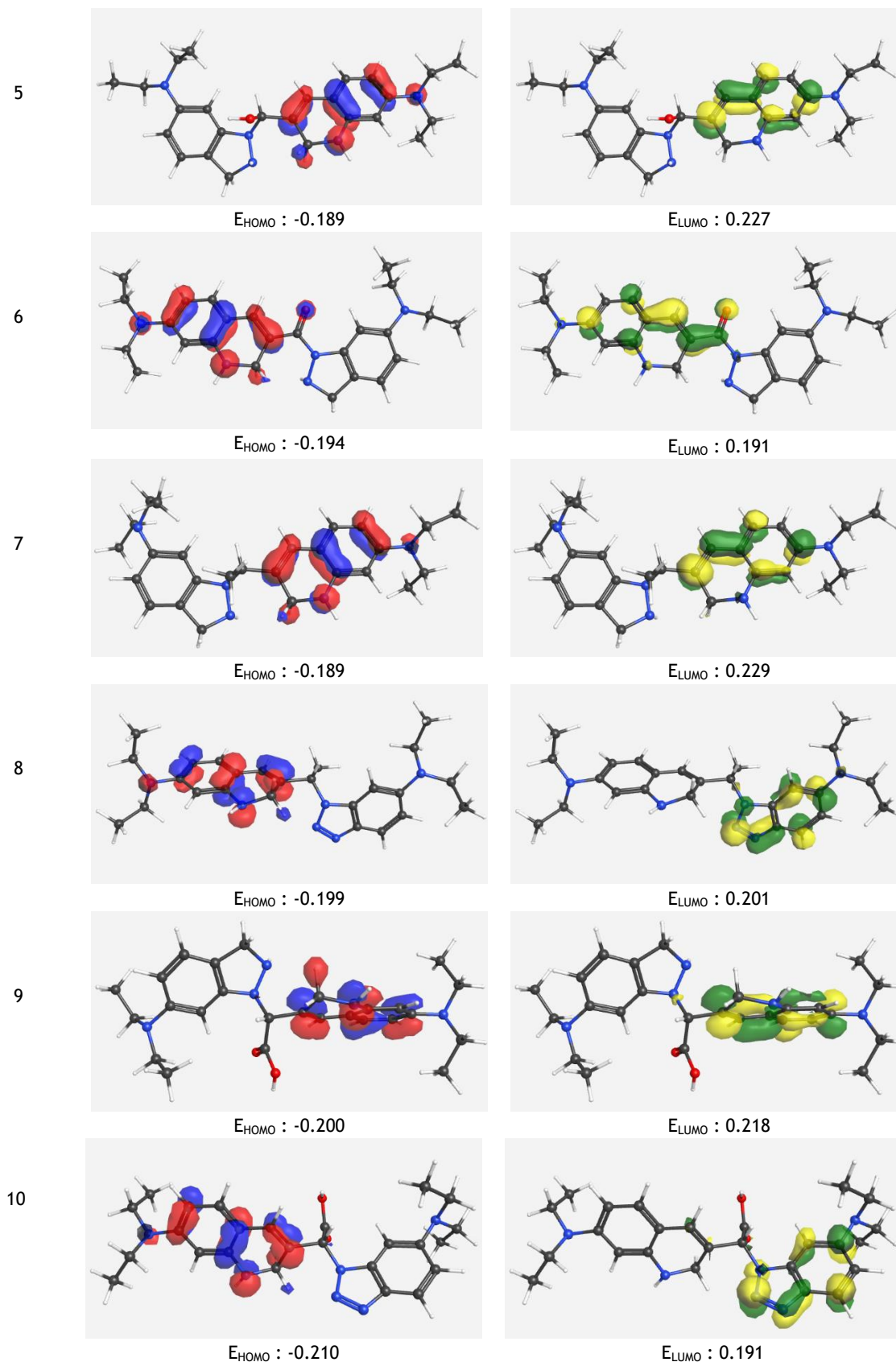
Fig. 19 (continued). Visual representation of E_{HOMO} and E_{LUMO} values for all molecules.

ΔE (E_{LUMO}-E_{HOMO}) is a critical parameter in predicting the chemical and physical behavior of molecules. This energy difference helps us understand the reactivity, stability, electronic and optical properties of the molecule. Since ΔE plays an important role in molecular design and analysis processes in chemistry, materials science, drug

development and many other fields, it has been calculated for related molecules. When the ΔE (E_{LUMO} - E_{HOMO}) values given in Table 11 are examined, it is seen that the lowest value belongs to molecule number 4 with 0.372 au and the highest value belongs to molecule number one with 0.422 au. Based on these results, we can say that molecule number 4 has the highest reactivity, the lowest stability, the

longest wavelength absorption, and the highest conductivity compared to other molecules. Molecule 1 has the lowest reactivity, the highest stability, the shortest wavelength absorption, and the lowest conductivity compared to the other molecules.

The ionization potential (IP) is an energy parameter that expresses the tendency of an atom or molecule to lose electrons. IP affects many chemical and physical properties such as chemical reactivity, electrical conductivity, spectral analyses and bond structure. Therefore, ionization potential is an important concept to predict the behavior of atoms and molecules and to make strategic decisions in various chemical applications. Molecule 2 has the lowest ionization potential (high reactivity, low stability, good conductivity, and tendency to form ionic bonds) with a value of 0.188 au, while molecule 10 has the highest ionization potential (low reactivity, high stability, high electronegativity and high electron attraction, and tendency to form covalent bonds) with a value of 0.210 au.

A high electron affinity (EA) indicates that the atom has a high tendency to accept electrons, making it stable. Among the molecules, molecule 4 has the highest electron affinity with -0.164 au. Low electron affinity, on the other hand, means that the atom does not need an electron from outside and is therefore stable or low reactive. Among the molecules, molecule number 7 has the lowest electron affinity with -0.229 au. Electron affinity varies according to the position of the elements in the periodic table and is an important parameter in understanding chemical reactivity.

Chemical potential (μ) is an important concept that determines a molecule's propensity to react, its energy state and its interaction with its environment. A high chemical potential indicates that the molecule has high reactivity and is more energy unstable. Among the molecules studied, molecule 4 was found to have the highest chemical potential with 0.022 au. Molecules with lower chemical potentials are more stable and less prone to reaction. Among the molecules studied, molecule 7 was found to have the lowest chemical potential with -0.020 au. Chemical potential is a critical parameter in understanding the behavior of systems in many fields such as equilibrium, diffusion, reaction engineering and electronics.

The global hardness (η) provides information about the molecule's reactivity, stability and tendency to accept/donate electrons. A high hardness indicates that the molecule is stable and less prone to undergo chemical reactions, while a low hardness indicates that the molecule is more reactive and can easily participate in electron transfer. Accordingly, molecule 4 has the lowest global hardness with 0.186 au, while molecule 1 has the highest global hardness with 0.211 au. Global hardness is an important parameter in understanding the chemical behavior and bonding properties of molecules.

Global softness (S) provides information about the molecule's chemical reactivity, polarizability and sensitivity to electron exchange. A high softness value indicates that the molecule is reactive, polarizable and prone to chemical interactions. When the data given in Table 11 are examined, it is determined that the highest global softness belongs to molecule 4 with a value of 2.688 au. A low softness value indicates that the molecule is stable and resistant to chemical changes. It was determined that the lowest global softness among the molecules belongs to molecule number 1 with a value of 2.370 au. Global softness is an important parameter in understanding the mechanisms of chemical reactions, catalysis and bonding tendencies.

Electrophilicity (ω) is an important parameter that indicates the reactivity of a molecule and its ability to attract electrons in interactions with other molecules. High electrophilicity indicates that the molecule is reactive and efficient at attracting electrons. The molecule with the highest electrophilicity among the molecules with a value of 0.001301075 au is molecule number 4. Low electrophilicity indicates that the molecule is less reactive and resistant to chemical interactions. The molecule with the lowest electrophilicity among the molecules with a value of 5.84416E-06 au is molecule 6. Electrophilicity plays an important role in understanding the chemical behavior of molecules and in drug design.

Table 11. Some quantum mechanical paramaters calculated for molecules.

Molecule	ΔE ($E_{LUMO}-E_{HOMO}$)	IP	EA	μ	η	S	ω
1	0.422	0.196	-0.226	-0.015	0.211	2.370	0.000533175
2	0.396	0.188	-0.208	-0.010	0.198	2.525	0.000252525
3	0.396	0.202	-0.194	0.004	0.198	2.525	4.04040E-05
4	0.372	0.208	-0.164	0.022	0.186	2.688	0.001301075
5	0.416	0.189	-0.227	-0.019	0.208	2.404	0.000867788
6	0.385	0.194	-0.191	0.002	0.193	2.597	5.84416E-06
7	0.418	0.189	-0.229	-0.020	0.209	2.392	0.000956938
8	0.400	0.199	-0.201	-0.001	0.200	2.500	0.000002500
9	0.418	0.200	-0.218	-0.009	0.209	2.392	0.000193780
10	0.401	0.210	-0.191	0.009	0.201	2.494	0.000225062

Self-Consistent Field (SCF) Energy is an important parameter that describes the behavior and energy state of the electrons of a molecule. A low SCF energy indicates that the molecule has a stable and non-reactive structure, while a high SCF energy indicates that the molecule is reactive and potentially unstable. When the data given in Table 12 are analyzed, it is determined that the molecule with the highest SCF energy is molecule number 10 with a Hartree value of -1433.5083607073 and the molecule with the lowest SCF energy is molecule number 1 with a Hartree value of -1232.2610262048. SCF energy is critical for the

Table 12. Self-Consistent Field (SCF) energy (Hartree) and dipole moment (Debye) calculated for molecules.

Molecule	Self-Consistent Field (SCF) Energy (Hartree)	Dipole Moment (Debye)
1	-1232.2610262048	3.3899
2	-1246.9616397020	3.7424
3	-1321.3891469613	5.9082
4	-1320.2288880406	3.0115
5	-1306.7027599666	3.7679
6	-1305.5640653116	4.0485
7	-1271.0709263312	1.9556
8	-1285.7856174193	5.4665
9	-1418.8056487774	2.6397
10	-1433.5083607073	2.4420

analysis of molecular structure and studies on chemical reactivity.

The dipole moment is an important physical parameter that describes the electrical polarity of a molecule and the direction of this polarity. A high dipole moment indicates that the molecule is polar and shows stronger intermolecular interactions. The highest dipole moment among the molecules belongs to molecule 3 with 5.9082 Debye. A low dipole moment indicates apolar character and weak interactions. The lowest dipole moment among the molecules belongs to molecule 7 with 1.9556 Debye. Dipole moment plays a critical role in understanding the chemical reactivity, solubility properties and spectral behavior of molecules.As a result of all these studies, (7-(diethylamino)-1,2-dihydroquinolin-3-yl) (6-(diethylamino)-2,3-dihydro-1H-indazol-1-yl)methanone (molecule 6) was determined as the ideal molecule. After this determination, in order to obtain more information about the open structure of the molecule, the open molecular formula of the molecule was first formed. This structure is given in Figure 20. Based on this molecular structure, bond lengths, bond angles, Mulliken atomic charge values of the ideal molecule were also calculated according to DFT methods on the basis set of B3LYP 6-311+G(2d,p) with the Gaussian 09W program. The obtained data are given in Table 13-15. Finally, molecular electrostatic potential (MEP) map was created to see the electron density in the final molecule. The related visualisation is also given in Figure 21. MEP represents the electrical properties and charge distribution of a molecule. MEP plays a critical role in understanding the polarity, reactivity and interactions of molecules. It helps to understand the interactions between molecular structures and provides important information in explaining chemical reaction mechanisms and charge exchanges. MEP is an important tool in the fields of chemical design and molecular modeling.
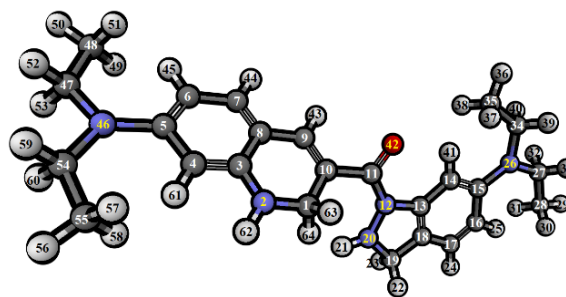
Fig. 20. Structural molecule formula of molecule number 6.

Table 13. The calculated bond lenghts (Å) of molecule 6 as DFT methods on the basis set of B3LYP 6-311+G(2d,p).

Sequence	Atoms	Bond Lenghts (Å)	Sequence	Atoms	Bond Lenghts (Å)
1	C(48)-C(47)	1.539	35	C(48)-H(49)	1.114
2	C(47)-N(46)	1.463	36	C(48)-H(50)	1.116
3	N(46)-C(54)	1.454	37	C(48)-H(51)	1.117
4	C(54)-C(55)	1.542	38	C(47)-H(52)	1.119
5	N(46)-C(5)	1.399	39	C(48)-H(53)	1.116
6	C(5)=C(6)	1.346	40	C(54)-H(59)	1.115
7	C(6)-C(7)	1.336	41	C(54)-H(60)	1.119
8	C(7)=H(8)	1.342	42	C(55)-H(57)	1.115
9	C(8)-C(3)	1.343	43	C(55)-H(58)	1.113
10	C(3)=C(4)	1.345	44	C(55)-H(56)	1.114
11	C(4)-C(5)	1.349	45	C(6)-H(45)	1.102
12	C(8)-C(9)	1.344	46	C(7)-H(44)	1.102
13	C(9)=C(10)	1.347	47	C(4)-H(61)	1.100
14	C(10)-C(1)	1.514	48	C(9)-H(43)	1.101
15	C(1)-N(2)	1.444	49	N(2)-H(62)	1.018
16	N(2)-C(3)	1.382	50	C(1)-H(63)	1.113
17	C(10)-C(11)	1.372	51	C(1)-H(64)	1.115

18	C(11)=O(42)	1.209	52	N(20)-H(21)	1.021
19	C(11)-N(12)	1.397	53	C(19)-H(23)	1.116
20	N(12-N(20	1.394	54	C(19)-H(22)	1.115
21	N(20)-C(19)	1.447	55	C(14)-H(41)	1.093
22	C(19)-C(18)	1.492	56	C(16)-H(25)	1.099
23	C(18)=C(13)	1.331	57	C(17)-H(24)	1.104
24	C(13)-N(12)	1.426	58	C(28)-H(29)	1.116
25	C(13)-C(14)	1.340	59	C(28)-H(30)	1.115
26	C(14)=C(15)	1.354	60	C(28)-H(31)	1.114
27	C(15)-C(16)	1.356	61	C(27)-H(32)	1.114
28	C(16)=C(17)	1.342	62	C(27)-H(33)	1.115
29	C(17)-C(18)	1.334	63	C(34)-H(39)	1.117
30	C(15)-N(26)	1.412	64	C(34)-H(40)	1.113
31	N(26)-C(34)	1.462	65	C(35)-H(36)	1.118
32	C(34)-C(35)	1.543	66	C(35)-H(37)	1.116
33	N(26)-C(27)	1.460	67	C(35)-H(38)	1.114
34	C(27)-C(28)	1.541			

Bond length refers to the center-to-center (nucleus) distance between two atoms. Bond lengths determine the strength and nature of interactions between atoms within the molecule. Short bond lengths generally represent stronger bonds, indicate that electrons interact more intensively, contribute to the overall stability of the molecule, can cause the molecule to be less reactive and increase the stability of the molecular structure. Short bond lengths mean a closer sharing of electrons between atoms. This can indicate that the bond may be more polar or ionic and can affect molecular geometry. When the bond lengths of our molecule number 6, which we determined as the ideal molecule in this study, are examined in Table 13, it is determined that the longest bond is between C(34)-C(35) atoms with 1.543 Å. Longer bond lengths generally represent weaker bonds. Single bonds (C-C) are usually longer and less strong. This means that the bond between atoms is less stable. Long bonds usually indicate more reactive molecules. Weak bonds can be easily broken and are more prone to participate in chemical reactions. Long bond lengths can increase the mobility of atoms within the molecule. Weaker bonds allow atoms to move more freely, which can affect the dynamic properties of the molecule. At the same time, longer bonds indicate that the molecule may be less polar. Ionic or non-polar bonds are generally longer. The shortest bond in the studied molecules was determined to be between N(2)-H(62) atoms with 1.018 Å.

Table 14. The calculated bond angles (°) of molecule 6 as DFT methods on the basis set of B3LYP 6-311+G(2d,p).

Seq.	Atoms	Bond Angles (°)	Seq.	Atoms	Bond Angles (°)
1	H(49)-C(48)-H(51)	106.054	62	C(10)-C(11)=O(42)	120.296
2	H(49)-C(48)-H(50)	108.631	63	C(10)-C(11)-N(12)	119.961
3	H(49)-C(48)-C(47)	112.100	64	O(42)=C(11)-N(12)	119.710
4	H(51)-C(48)-H(50)	107.695	65	C(11)-N(12)-N(20)	125.949
5	H(51)-C(48)-C(47)	111.120	66	C(11)-N(12)-C(13)	121.575
6	H(50)-C(48)-C(47)	111.014	67	N(12)-N(20)-H(21)	104.390
7	C(48)-C(47)-H(52)	106.883	68	N(12)-N(20)-C(19)	104.992
8	C(48)-C(47)-H(53)	109.888	69	H(21)-N(20)-C(19)	110.431
9	C(48)-C(47)-N(46)	113.487	70	C(11)-N(12)-C(13)	121.575
10	H(52)-C(47)-H(53)	104.880	71	N(20)-C(19)-H(22)	109.862
11	H(52)-C(47)-N(46)	109.646	72	N(20)-C(19)-H(23)	110.307
12	H(53)-C(47)-N(46)	111.595	73	N(20)-C(19)-C(18)	104.760
13	C(47)-N(46)-C(54)	114.472	74	N(20)-N(12)-C(13)	112.167
14	C(47)-N(46)-C(5)	110.718	75	H(22)-C(19)-H(23)	110.576
15	N(46)-C(54)-H(59)	108.899	76	H(22)-C(19)-C(18)	110.097
16	N(46)-C(54)-H(60)	110.538	77	H(23)-C(19)-C(18)	111.091
17	N(46)-C(54)-C(55)	113.789	78	C(19)-C(18)=C(13)	110.689
18	H(59)-C(54)-H(60)	105.519	79	C(19)-C(18)-C(17)	128.987
19	H(59)-C(54)-C(55)	106.224	80	C(18)=C(13)-N(12)	106.121
20	H(60)-C(54)-C(55)	111.414	81	C(18)=C(13)-C(14)	120.404
21	C(54)-C(55)-H(58)	109.922	82	C(13)=C(18)-C(17)	120.316
22	C(54)-C(55)-H(57)	114.659	83	N(12)-C(13)-C(14)	133.468

|					
23	C(54)-C(55)-H(56)	109.922	84	C(18)-C(17)-H(24)	119.981
24	H(56)-C(55)-H(57)	106.079	85	C(18)-C(17)=C(16)	118.125
25	H(56)-C(55)-H(58)	107.893	86	H(24)-C(17)=C(16)	121.874
26	H(57)-C(55)-H(58)	106.632	87	C(17)=C(16)-C(15)	124.150
27	C(54)-N(46)-C(5)	116.295	88	C(17)=C(16)-H(25)	114.233
28	N(46)-C(5)-C(4)	124.716	89	H(25)-C(16)-C(15)	121.614
29	N(46)-C(5)=C(6)	119.588	90	C(16)-C(15)=C(14)	114.919
30	C(5)=C(6)=H(46)	120.450	91	C(16)-C(15)-N(26)	121.838
31	C(5)-C(4)-H(61)	120.008	92	C(14)=C(15)-N(26)	123.239
32	C(5)=C(6)-C(7)	121.888	93	H(41)-C(14)=C(15)	119.641
33	H(45)-C(6)-C(7)	117.652	94	H(41)-C(14)-C(13)	118.313
34	C(6)-C(7)-H(44)	118.117	95	C(15)=C(14)-C(13)	122.023
35	C(6)-C(7)=C(8)	120.845	96	C(15)-N(26)-C(27)	115.925
36	H(44)-C(7)=C(8)	121.004	97	C(15)-N(26)-C(34)	118.598
37	C(7)=C(8)-C(9)	119.464	98	N(26)-C(27)-C(28)	112.849
38	C(7)=C(8)-C(3)	119.256	99	N(26)-C(34)-C(35)	114.161
39	C(8)-C(3)=C(4)	118.363	100	H(29)-C(28)-H(30)	107.488
40	C(8)-C(3)-N(2)	121.711	101	H(29)-C(28)-H(31)	106.947
41	C(3)=C(4)-C(5)	123.888	102	H(30)-C(28)-H(31)	107.845
42	C(3)=C(4)-H(61)	116.102	103	H(29)-C(28)-C(27)	110.795
43	C(4)-C(5)=C(6)	115.682	104	H(30)-C(28)-C(27)	109.944
44	C(4)=C(3)-N(2)	119.901	105	H(31)-C(28)-C(27)	113.580
45	C(8)-C(9)-H(43)	116.287	106	C(28)-C(27)-H(33)	106.668
46	C(8)-C(9)=C(10)	122.942	107	C(28)-C(27)-H(32)	112.181
47	C(9)=C(10)-C(1)	116.867	108	H(33)-C(27)-N(26)	111.870
48	H(43)-C(9)=C(10)	120.739	109	H(32)-C(27)-N(26)	110.641
49	C(9)=C(10)-C(11)	115.349	110	C(27)-N(26)-C(34)	115.814
50	C(10)-C(1)-H(63)	111.209	111	N(26)-C(34)-H(39)	110.148
51	C(10)-C(1)-H(64)	108.559	112	N(26)-C(34)-H(40)	111.703
52	C(10)-C(1)-N(2)	114.795	113	H(32)-C(27)-H(33)	102.071
53	H(63)-C(1)-H(64)	110.102	114	H(39)-C(34)-C(35)	104.587
54	H(63)-C(1)-N(2)	104.954	115	H(40)-C(34)-C(35)	111.942
55	H(64)-C(1)-N(2)	107.085	116	H(39)-C(34)-H(40)	103.499
56	C(1)-N(2)-H(62)	114.549	117	C(34)-C(35)-H(36)	111.197
57	C(1)-N(2)-C(3)	116.734	117	C(34)-C(35)-H(37)	114.088
58	H(62)-N(2)-C(3)	112.765	119	C(34)-C(35)-H(38)	110.133
59	N(2)-C(3)-C(8)	121.711	120	H(36)-C(35)-H(37)	107.382
60	C(3)-C(8)-C(9)	121.281	121	H(36)-C(35)-H(38)	107.688
61	C(1)-C(10)-C(11)	127.570	122	H(37)-C(35)-H(38)	106.030

Bond angle refers to the angle formed by two bonds within a molecule. It is usually measured by considering the center of one atom, the position of the two bonded atoms. Bond angles play a critical role in determining the overall shape of the molecule. Large bond angles indicate that the molecule is more angular, stable and generally less reactive, can reduce steric dispute and allow for a more even distribution of electrons, and are usually associated with molecules that exhibit apolar properties. When the bond angles given in Table 14 are examined, it is determined that the largest head angle is between C(1)-C(10)-C(11) atoms with 127.570˚. Small bond angles indicates that the molecule has a tighter and denser structure, which means it can be more reactive. It can also increase steric dispute and facilitate certain chemical reactions and is often associated with molecules that exhibit polar properties. When the bond angles of number 6 were analyzed, it was observed that the narrowest angle was between H(32)-C(27)-H(33) atoms with 102.071 ˚.

Mulliken atomic charge values are based on the electron density of the atoms of a molecule and represent the interatomic charge distribution. These values are widely used, especially in quantum chemistry and molecular modeling. Since Mulliken charges are important for evaluating the interactions of atoms with electrons and the charge distribution within the molecule, Mulliken Atomic Charge Values of molecule 6 are given in Table 15.

Table 15. Mulliken atomic charge values of the molecule 6 as DFT methods on the basis set of B3LYP 6-311+G(2d,p).

Sequence	Atoms	Charge (a.u)	Sequence	Atoms	Charge (a.u)
1	C	-0.101029	33	H	0.201347
2	N	-0.939598	34	C	-0.170939
3	C	0.423909	35	C	-0.580727
4	C	-0.230061	36	H	0.202587
5	C	0.312886	37	H	0.233839
6	C	-0.229210	38	H	0.185104
7	C	-0.177497	39	H	0.187020
8	C	-0.176281	40	H	0.213611
9	C	-0.014884	41	H	0.296633
10	C	-0.266859	42	O	-0.663411
11	C	0.951585	43	H	0.289612
12	N	-0.897147	44	H	0.246940
13	C	0.461976	45	H	0.244943
14	C	-0.193647	46	N	-0.822788
15	C	0.335921	47	C	-0.185876
16	C	-0.223532	48	C	-0.571509
17	C	-0.240045	49	H	0.204272
18	C	-0.213021	50	H	0.207812
19	C	-0.117046	51	H	0.187693
20	N	-0.475493	52	H	0.207186
21	H	0.328581	53	H	0.200931
22	H	0.220303	54	C	-0.165936
23	H	0.237870	55	C	-0.586839
24	H	0.234555	56	H	0.211216
25	H	0.249905	57	H	0.217040
26	N	-0.854896	58	H	0.187336
27	C	-0.177292	59	H	0.175870
28	C	-0.590911	60	H	0.216644
29	H	0.190515	61	H	0.228604
30	H	0.189270	62	H	0.326741
31	H	0.222235	63	H	0.199983
32	H	0.210793	64	H	0.223208
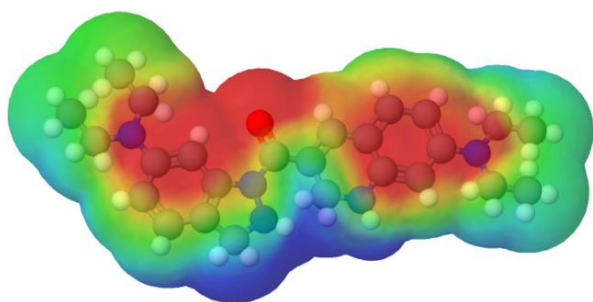
Fig. 21. Molecular electrostatic potential (MEP) for molecule 6.

4. Conclusion

Among the ten different 1,2-dihydroquinoline derivative compounds I considered in this study, molecule 6 ((7-(diethylamino)-1,2-dihydroquinolin-3-yl)(6-(diethyl-amino)-2,3-dihydro-1H-indazol-1-yl)methanone) gave the highest docking score with 7TD4-coded protein among the target proteins I identified. With the other 3PP4, 6OBD, and 7YXA-coded proteins, the highest docking score was also obtained with molecule 6. The fact that molecule 6

crossed the blood-brain barrier (BBB) in the BOILED-Egg graphic and especially that the entire red line in the bioavailability radar graphic was within the pink area (giving successful results in all six parameters) showed us that this molecule could be an ideal drug substance. Apart from these, the lipophilicity, water solubility, pharmacokinetics properties, druglikeness and medicinal chemistry, bioactivity, toxicity risks, drug- scores, and quantum mechanical parameter properties examined also showed us that this molecule is a molecule that can be used as a drug-active ingredient in the treatment of MS. I believe that our theoretical study can be supported by experimental studies, and an upper-phase study can be started at the point of drug development.

References

1. Taghour, M.S.; Elkady, H.; Eldehna, W.M.; El-Deeb, N.M.; Kenawy, A.M.; Elkaeed, E.B.; Alsfouk, A.A; Alesawy, M.S.; Metwaly, A.M.; Eissa, I.H. Design and synthesis of thiazolidine-2,4-diones hybrids with 1,2-dihydroquinolones and 2-oxindoles as potential VEGFR-2 inhibitors: in-vitro anticancer evaluation and in-silico studies. *J. Enzyme Inhib. Med. Chem.* **2022**, *37*(1), 1903-1917. https://doi.org/10.1080/14756366. 2022.2085693

2. Alzweiri, M.; Sweidan, K.; Saleh, O.A.; Al-Helo, T. Synthesis and evaluation of new 2-oxo-1,2-dihydroquinoline-3-carboxamides as potent inhibitors against acetylcholinesterase enzyme. *Med. Chem. Res.* **2022**, *31*(9), 1448-1460. https://doi.org/ 10.1007/s00044-022-02922-x

3. Huddar, S.; Park, C.M.; Kim, H.J.; Jang, S.; Lee, S. Discovery of 4-hydroxy-2-oxo-1,2-dihydroquinolines as potential inhibitors of Streptococcus pneumoniae, including drug-resistant strains. *Bioorg. Med. Chem. Lett.* **2020**, *30*(9), 127071-127074. https://doi.org/ 10.1016/j.bmcl.2020.127071

4. Shahin, M.I.; Roy, J.; Hanafi, M.; Wang, D.; Luesakul, U.; Chai, Y.; Muangsin, N.; Lasheen, D.S.; El Ella, D.A.A; Abouzid, K.A.; Neamati, N. Synthesis and biological evaluation of novel 2-oxo-1,2-dihydroquinoline-4-carboxamide derivatives for the treatment of esophageal squamous cell carcinoma. *Eur. J. Med. Chem.* **2018**, *155*, 516-530. https://doi.org/10.1016/j.ejmech.2018.05.042

5. Banu, S.; Bollu, R.; Naseema, M.; Gomedhika, P.M.; Nagarapu, L.; Sirisha, K.; Kumar, C.G.; Gundasw, S.K. A novel templates of piperazinyl-1,2-dihydroquinoline-3-carboxylates: Synthesis, anti-microbial evaluation and molecular docking studies. *Bioorg. Med. Chem. Lett.* **2018**, *28*(7), 1166-1170. https://doi.org/ 10.1016/j.bmcl.2018.03.007

6. Agwupuye, J.A.; Gber, T.E.; Edet, H.O.; Zeeshan, M.; Batool, S.; Duke, O.E.E.; Adah, P.O.; Odey, J.O.; Egbung, G.E. Molecular modeling, DFT studies and biological evaluation of methyl 2,8-dichloro-1,2-dihydroquinoline-3-carboxylate. *Chem. Phys. Impact.* **2023**, *6*, 100146-100157. https://doi.org/10.1016/j.chphi.2022.100146

7. Hayani, S.; Sert, Y.; Filali, Y.; Benhiba, F.; Chahdi, F.O.; Laraqui, F.Z.; Mague, J.T.; Ibrahimi, B.E.; Sebbar, N.K.; Rodi, Y.K.; Essassi, E.M. New alkyl (cyclohexyl) 2-oxo-1-(prop-2-yn-1-yl)-1,2-dihydroquinoline-4-carboxylates: Synthesis, crystal structure, spectroscopic characterization, hirshfeld surface analysis, molecular docking studies and DFT calculations. *J. Mol. Struct.* **2021**, *1227*, 129520-129534. https://doi.org/10.1016/j.molstruc.2020.129520

8. Baltina, L.A.; Fairushina, A.I.; Baltina, L.A.; Eropkin, M.Y.; Konovalova, N.I.; Petrova, P.A.; Eropkina, E.M. Eropkina, EM (Eropkina, E. M.), Synthesis and antiviral activity of glycyrrhizic-acid conjugates with aromatic amino acids. *Chem. Nat. Compd.* **2022**, *53*(6), 1096-1100. https://doi.org/ 10.1007/s10600-017-2209-7

9. Gaber, A.; Alsanie, W.F.; Alhomrani, M.; Alamri, A.S.; El-Deen, I.M.; Refat, M.S. Synthesis of 1-[(Aryl) (3-amino-5-oxopyrazolidin-4-ylidene)methyl]-2-oxo-1,2-dihydroquinoline-3-carboxylic acid derivatives and their breast anticancer activity. *Crystals* **2021**, *11*(5), 571-582. https://doi.org/ 1096-1100.10.3390/ cryst11050571

10. Kryl'skii, E.D.; Kravtsova, S.E.; Popova, T.N.; Matasova, L.V.; Shikhaliev, K.S.; Medvedeva S.M. 6-Hydroxy-2,2,4-trimethyl-1,2-dihydroquinoline demonstrates anti-inflammatory properties and reduces oxidative stress in acetaminophen-induced liver injury in rats. *Curr. Issues Mol. Biol.* **2023**, *45*(10), 8321-8336. https://doi.org/10.3390/cimb45100525

11. Zidan, T.A.; Yehia, A.A. Novel antioxidants based on polymerized 2,2,4-trimethyl-1,2-dihydroquinoline for styrene-butadiene rubber composites. *J. Polym. Res.* **2024**, *31*(6), 170-185. https://doi.org/10.1007/ s10965-024-04006-3

12. Gorojankina, T.; Hoch, L.; Faure, H.; Roudaut, H.; Traiffort, E.; Schoenfelder, A.; Girard, N.; Mann, A.; Manetti, F.; Solinas, A.; Petricci, E.; Taddei, M.; Ruat, M. Discovery, Molecular and Pharmacological Characterization of GSA-10, a Novel Small-Molecule Positive Modulator of Smoothened. *Mol. Pharmacol.* **2013**, *83*(5), 1020-1029. https://doi.org/10.1124/mol.112.084590

13. Lee, C.H.; Jin, H.; Lee, J.H.; Cho, H.J.; Kim, J.; Chung, K.C.; Jung, S.; Paik, S.R. Dequalinium-induced protofibril formation of α-synuclein. *J. Biol. Chem.* **2006**, *281*(6), 3463-3472. https://doi.org/ 10.1074/jbc.M505307200.

14. Kim, H.; Kim, B.J.; Koh, S.; Cho, H.J.; Jin, X.; Kim, B.G.; Choi, J.Y. High mobility group box 1 in the central nervous system: regeneration hidden beneath inflammation. *Neural Regen. Res.* **2025**, *20*(1), 107-115. https://doi.org/10.4103/NRR.NRR-D-23-01964

15. Xue, Y.; Yin, P.; Chen, H.; Li, G.; Zhong, D. Novel peripheral blood mononuclear cell mRNA signature for IFN-beta therapy responsiveness prediction in multiple sclerosis. *Autoimmunity* **2024**, *57*(1), 1-12. https://doi.org/10.1080/08916934.2024.2332340

16. Leussink, V.I.; Jankovic, M.; Growth, M.; Schuh, K.; Sauerbeck, I.S.; Hoffmann, O. Addition of quantitative MRI to the routine clinical care of patients with multiple sclerosis-results from the MAGNON project. *Brain Behav.* **2024**, *14*(6), 1-11. https://doi.org/10.1002/brb3.3548

17. Diem, L.; Ovchinnikov, A.; Friedli, C.; Hammer, H.; Kamber, N.; Chan, A.; Salmen, A.; Findling, O.; Hoepner, R. Efficacy and safety of ocrelizumab in patients with relapsing multiple sclerosis: Real-world experience of two Swiss multiple sclerosis centers. *Mult. Scler. Relat. Disord.* **2024**, *86*, 1-7. https://doi.org/10.1016/j.msard.2024.105570

18. Hassan, S.S.; Darwish, E.S.S.; Ahmed, G.K.K.; Azmy, S.R.R.; Haridy, N.A.A. Relationship between disability and psychiatric outcome in multiple sclerosis patients and its determinants. *Egypt. J. Neurol. Psychiatry Neurosurg.* **2023**, *59*(1), 105-118. https://doi.org/10.1186/s41983-023-00702-x

19. Curran, C.; Vaitaitis, G.; Waid, D.; Volmer, T.; Alverez, E.; Wagner, D.H. Ocrevus reduces TH40 cells, a biomarker of systemic inflammation, in relapsing multiple sclerosis (RMS) and in progressive multiple sclerosis (PMS). *J. Neuroimmunol.* **2023**, *374*, 578008-578019. https://doi.org/10.1016/j.jneuroim.2022.578008

20. Rath, L.; Vijiaratnam, N.; Skibina, O. Alemtuzumab (Lemtrada) in multiple sclerosis: lessons from social media in enhancing patient care. *Mult. Scler. J.* **2016**, *22*(3), 335-355.

21. Uosef, A.; Vaughn, N.; Chu, X.; Elshawwaf, M.; Abdelshafy, A.A.A.; Elsaid, K.M.K.; Ghobrial, R.M.; Kloc, M. Siponimod (Mayzent) Downregulates RhoA and Cell Surface Expression of the S1P1 and CX3CR1 Receptors in Mouse RAW 264.7 Macrophages. *Arch. Immunol. Ther. Exp.* **2020**, *68*(3), 19-26. https://doi.org/10.1007/s00005-020-00584-4

22. Burley, S.K.; Berman, H.M.; Christie, C.; Duarte, J.M.; Feng, Z.; Westbrook, J.; Young, J.; Zardecki, C. RCSB Protein Data Bank: Sustaining a living digital data resource that enables breakthroughs in scientific research and biomedical education. *Protein Sci.* **2018**, *27*(1), 316-330. https://doi.org/10.1016/j.bpj.2018. 11.1783

23. Wang, Y.; Lu, J.; Xiao, H.; Ding, L.; He, Y.; Chang, C.; Wang, W. Mechanism of Valeriana Jatamansi Jones for the treatment of spinal cord injury based on network pharmacology and molecular docking. *Medicine* **2023**, *102*(50), 1-9. https://doi.org/10.1097/MD. 0000000000036434

24. Ni, X.; Bao, H.; Guo, J.; Li, D.; Wang, L.; Zhang, W.; Sun, G. Discussion on the mechanism of Danggui Sini decoction in treating diabetic foot based on network pharmacology and molecular docking and verification of the curative effect by meta-analysis. *Front. Endocrinol.* **2024**, 15, 1-14. https://doi.org/10.3389/fendo.2024.1347021

25. Loganathan, V.; Akbar, I.; Ahamed, A.; Alodaini, H.A.; Hatamleh, A.A.; Abuthkir, M.H.S.; Gurusamy, R. Synthesis, antimicrobial and cytotoxic activities of tetrazole N-Mannich base derivatives: Investigation of DFT calculation, molecular docking, and Swiss ADME studies. *J. Mol. Struct.* **2024**, *1300*, 1-13. https://doi.org/10.1016/j.molstruc.2023. 137239

26. Jarupula, V.; Kumar, E.P.; Bujji, S.; Shivarathri, P.; Neeradi, S.; Morthad, M.; Reddy, K.L. Synthesis of novel hybrids containing 1,2,3-triazole-linked tetrazole moieties, evaluation of anticancer activity and molecular docking studies. *Russ. J. Gen. Chem.* **2023**, *93*(4), 849-857. https://doi.org/10.1134/S1070363223170012

27. Ganjo, A.R.; Adham, A.N.; Al-Bustany, H.A.; Aka, S.T. Phytochemical analysis and evaluation of antibacterial activity of *Moringa oleifera* extracts against gram-negative bacteria: an in vitro and molecular docking studies. *Curr. Issues Pharm. Med. Sci.* **2022**, *35*(4), 198-205. https://doi.org/10.2478/cipms-2022-0035

28. Daina, A.; Michielin, O.; Zoete, V. SwissADME: a free web tool to evaluate pharmacokinetics, drug-likeness, and medicinal chemistry friendliness of small molecules. *Sci. Rep.* **2017**, *7*(42717), 1-13. https://doi.org/10.1038/srep42717

29. Pirzada, A.S.; Khan, H.; Alam, W.; Darwish, H.W.; Elhenawy, A.A.; Kuznetsov, A.; Daglia, M. Physicochemical properties, pharmacokinetic studies, DFT approach, and antioxidant activity of nitro and chloro indolinone derivatives. *Front. Chem.* **2024**, *12*, 1-15. https://doi.org/10.3389/fchem.2024.1360719

30. Yousuf, M. Advances in in-silico based predictive in-vivo profiling of novel potent β-glucuronidase inhibitors. *Curr. Cancer Drug Targets* **2019**, *19*(11), 906-918. https://doi.org/10.2174/15680096196661 90320102238

31. Kumar, A.S.; Bhaskara, B.L. Computational and spectral studies of 3,3′-(propane-1,3-diyl) bis(7,8-dimethoxy-1,3,4,5-tetrahydro-2H-benzo[d]azepin-2-one). *Heliyon* **2019**, *5*(9), 1-10. https://doi.org/10.1016/j.heliyon.2019.e02420

32. Morak-Mlodawska, B.; Jelen, M.; Martula, E.; Korlacki, R. Study of lipophilicity and adme properties of 1,9-diazaphenothiazines with anticancer action. *Int. J. Mol. Sci.* **2023**, *24*(8), 6970-6981.https://doi.org/ 10.3390/ijms24086970

33. Islamoğlu, F.; Hacıfazlıoğlu, E. Investigation of the usability of some triazole derivative compounds as drug active ingredients by adme and molecular docking properties. *Mor. J. Chem.* **2022**, *10*(4), 861-880. https://doi.org/10.48317/IMIST.PRSM/morjchem-v10i3.30855

34. Kuchana, M.; Kaparthi, K. Prediction of physicochemical properties, bioactivity, pharmacokinetics, drug-likeness and synthetic accessibility of phenyl and isoxazole azo dyes. *Biosci. Biotechnol. Res. Commun.* **2021**, *14*(5), 301-305. https://doi.org/10.21786/bbrc/14.5/53.

35. Al-Warhi, T.; Said, M.A.; El Hassab, M.A.; Aljaeed, N.; Ghabour, H.A.; Almahli, H.; Eldehna, W.M.; Abdel-Aziz, H.A. Unexpected synthesis, single-crystal x-ray structure, anticancer activity, and molecular docking studies of certain 2-((imidazole/benzimidazol-2-yl)thio)- 1-arylethanon es. *Crystals* **2020**, *10*(6), 446-464. https://doi. org/10.3390/cryst10060446

36. Yussoff, M.A.M.; Hamid, A.A.A.; Hamid, S.A.; Halim, K.B.A. Computational quest for finding potential ebola vp40 inhibitors: a molecular docking study. *Sains Malays.* **2020**, 49(3), 537-544. https://doi.org/10.17576/jsm-2020-4903-08

37. Prabha, B.; Ezhilarasi, M.R. Synthesis, spectral characterization, in vitro and in silico studies of benzodioxin pyrazoline derivatives. *Biointerface Res. Appl. Chem.* **2021**, *11*(2), 9126-9138. https://doi.org/10.33263/BRIAC112.91269138

38. Ahn, S.; Truong, V.N.P.; Kim, B.; Yoo, M.; Lim, Y.; Cho, S.K.; Koh, D. Design, synthesis, and biological evaluation of chalcones for anticancer properties targeting glycogen synthase kinase 3 beta. *Appl. Biol. Chem.* **2022**, *65*(17), 1-14. https://doi.org/10.1186/s13765-022-00686-x

39. Singh, S.; Gupta, A.K.; Chattree, A.; Verma, A. Lead finding from whole plant of curcuma longa with

oxidative potential. *Int. J. Pharm. Sci. Res.* **2013**, *4*(8), 3142-3146. https://doi.org/10.13040/IJPSR. 0975-8232.4(8).3142-46

40. Silva, Y.K.C.; Reyes, C.T.M.; Rivera, G.; Alves, M.A.; Barreiro, E.J.; Moreira, M.S.A.; Lima, L.M. 3-aminothiophene-2-acylhydrazones: non-toxic, analgesic and anti-inflammatory lead-candidates. *Molecules* **2014**, *19*(6), 8456-8471. https://doi.org /10.3390/molecules19068456

41. Vaugelade, S.D.; Nicol, E.; Vujovic, S.; Bourcier, S.; Pirnay, S.; Bouchonnet, S. UV-vis degradation of α-tocopherol in a model system and in a cosmetic emulsion-Structural elucidation of photoproducts and toxicological consequences. *J. Chromatogr. A.* **2017**, *1517*, 126-133. https://doi.org/10.1016/j.chroma. 2017.08.015

42. Sharma, D.; Thakur, A.; Sharma, M.K.; Sharma, R.; Kumar, S.; Sihmar, A.; Dahiya, H.; Jhaa, G.; Kumar, A.; Sharma, A.K.; Om, H. Effective corrosion inhibition of mild steel using novel 1,3,4-oxadiazole--pyridine hybrids: Synthesis, electrochemical, morphological, and computational insights. *Environ. Res.* **2023**, *234*(116555), 1-21. https://doi.org/10.1016/j. envres. 2023.116555